

Regulated Expression of the Prostacyclin Receptor (IP) Gene by Androgens within the Vasculature: Combined role for Androgens and Serum Cholesterol. Eivers SB & Kinsella BT. (2016) *Biochim Biophys Acta (Gene Regulatory Mechanisms)*, **1859(10)**, p1333-1351.

## **Regulated Expression of the Prostacyclin Receptor (IP) Gene by Androgens within the Vasculature: Combined role for Androgens and Serum Cholesterol**

Sarah B. Eivers and B. Therese Kinsella\*

UCD School of Biomolecular and Biomedical Sciences, UCD Conway Institute of Biomolecular and Biomedical Research, University College Dublin, Belfield, Dublin 4, Ireland

Corresponding author Tel: 353-1-7166727; Fax: 353-1-7166456; Email: [therese.kinsella@ucd.ie](mailto:therese.kinsella@ucd.ie)

**Running title:** Regulation of the PTGIR by androgens

**Key words:** Prostacyclin receptor, gene expression, promoter, androgen response element (ARE)

**Abbreviations:** AA, arachidonic acid; ActD, actinomycin D; ADT, androgen deprivation therapy; AR, androgen receptor; ARE, androgen response element; ARR, androgen responsive region; bHLH-LZ, basic helix-loop-helix leucine zipper; BIC, bicalutamide; CHIP, chromatin immunoprecipitation; CHO, cholesterol; CHX, cycloheximide; COX, cyclooxygenase; CSS, charcoal stripped serum; CVD, cardiovascular disease; DAPI, 4'-6-diamidino-2-phenylindole; DHT, 5 $\alpha$ -dihydrotestosterone; E<sub>2</sub>, estrogen; ER, estrogen receptor; ERE, estrogen response element; ENZ, enzalutamide; FBS, fetal bovine serum; GPCR, G-protein coupled receptor; HEL, human erythroleukemia; HF, hydroxyflutamide; hIP, human I prostanoid receptor/prostacyclin receptor; 1<sup>o</sup>HUVECs, primary human umbilical vein endothelial cells; IP, I prostanoid receptor; LCS, low cholesterol serum; NS, normal serum; PGI<sub>2</sub>, prostaglandin I<sub>2</sub>; PGIS, prostacyclin synthase; PK, protein kinase; PrmIP, hIP promoter; PTGIR, hIP gene; qRT-PCR, quantitative reverse-transcriptase PCR; SCAP, SREBP cleavage activating protein; SREBP, sterol regulatory element binding protein; SRE, sterol response element.

## 1. Abstract

The prostanoid prostacyclin plays a key cardioprotective role within the vasculature. There is increasing evidence that androgens may also confer cardioprotection but through unknown mechanisms. This study investigated whether the androgen dihydrotestosterone (DHT) may regulate expression of the prostacyclin/I prostanoid receptor or, in short, the IP in platelet-progenitor megakaryoblastic and vascular endothelial cells. DHT significantly increased IP mRNA and protein expression, IP-induced cAMP generation and promoter (PrmIP)-directed gene expression in all cell types examined. The androgen-responsive region was localized to a *cis*-acting androgen response element (ARE), which lies in close proximity to a functional sterol response element (SRE) within the core promoter. In normal serum conditions, DHT increased IP expression through classic androgen receptor (AR) binding to the functional ARE within the PrmIP. However, under conditions of low-cholesterol, DHT led to further increases in IP expression through an indirect mechanism involving AR-dependent upregulation of SCAP expression and enhanced SREBP1 processing & binding to the SRE within the PrmIP. Chromatin immunoprecipitation assays confirmed DHT-induced AR binding to the ARE *in vivo* in cells cultured in normal serum while, in conditions of low cholesterol, DHT led to increased AR and SREBP1 binding to the functional ARE and SRE *cis*-acting elements, respectively, within the core PrmIP resulting in further increases in IP expression. Collectively, these data establish that the human IP gene is under the transcriptional regulation of DHT, where this regulation is further influenced by serum-cholesterol levels. This may explain, in part, some of the protective actions of androgens within the vasculature.

**Acknowledgements:** We thank Dr Helen M. Reid for reading the manuscript during its preparation. This work was supported by the Programme for Research in Third Level Institutions (PRTL; MolCellBiol) and the European Regional Development Fund and by an Irish Cancer Society Research Award, co-funded by the Health Research Board in Ireland and the Movember Foundation (Grant no. PCI12KIN (MRCG/2012/3)). In respect of conflict of interests, the authors declare that they have no competing interests.

## 2. Introduction

The prostanoid prostacyclin, or prostaglandin (PG)<sub>I<sub>2</sub></sub>, is synthesized from arachidonic acid (AA) by the sequential actions of cyclooxygenase (COX)<sub>1/2</sub> and prostacyclin synthase (PGIS) mainly within the vascular endothelium and smooth muscle [1]. Prostacyclin predominantly signals through its cognate I Prostanoid receptor or, in short, the IP, a G protein coupled receptor (GPCR) primarily coupled to G<sub>s</sub>-mediated activation of adenylyl cyclase, increasing cellular cAMP levels [2, 3]. The protective role of prostacyclin within the vasculature is well documented, where it largely counteracts the actions of the pro-thrombotic prostanoid thromboxane (TX)<sub>A<sub>2</sub></sub> inhibiting platelet activation/aggregation while also acting as a potent vasodilator, and promotes re-endothelialisation/blood vessel repair in response to injury [4]. Imbalances in the levels of prostacyclin, or of its synthase or its receptor, the IP, have been implicated in several cardiovascular diseases (CVDs) including atherothrombosis, thrombotic stroke, myocardial infarction and in pulmonary arterial hypertension [5-7]. Furthermore, several single nucleotide polymorphisms occur within the human IP gene, the PTGIR, that correlate with receptor dysfunction including enhanced platelet activation in deep vein thrombosis and increased intimal hyperplasia, accelerating atherothrombotic events [8, 9]. The cardioprotective role of the prostacyclin/IP axis is also highlighted in mouse model systems. For example, IP<sup>-/-</sup> mice display increased incidence of occlusive thrombi and enhanced predisposition towards atherosclerosis and restenosis compared to wild type mice [10, 11]. Moreover, endothelial progenitor cells (EPCs) from IP<sup>-/-</sup> mice fail to promote re-endothelialisation/vessel repair in mice challenged with wire-induced vessel injury, highlighting the central role of the prostacyclin-IP axis in limiting neointimal hyperplasia/restenosis following endothelial injury [12].

Given the significant protective roles of the IP in the vasculature, identifying the factors that regulate expression of the human IP receptor gene (the PTGIR) is of significant interest to understanding the etiology and/or predisposition to such vascular diseases [13]. In addition to prostacyclin, the benefits of low serum cholesterol in protecting against CVDs are widely accepted. Indeed, some of the benefits of low serum cholesterol have been partly attributed to its influence on prostacyclin within the vasculature [14]. For example, reductions in LDL-cholesterol increases prostacyclin generation in endothelial cells (ECs) and occurs through the transcriptional upregulation of COX<sub>2</sub>, but not COX<sub>1</sub> or PGIS, by binding of the cholesterol-responsive transcription factor sterol response element binding protein (SREBP) 1 to a sterol response element (SRE) within the COX<sub>2</sub> promoter [15]. Moreover, and consistent with this, reduced serum cholesterol can also increase PTGIR/IP expression and function within the vasculature and this occurs through a similar transcriptional mechanism involving direct binding of the cholesterol-responsive SREBP1 to a conserved *cis*-acting SRE within the core promoter region of the PTGIR gene [16].

Marked differences occur in the age-of-onset and risk of developing CVD between men and women, where women will typically exhibit cardiovascular problems approximately 10 years later than men. Such gender-related differences in the rate of occurrence of CVD has been largely attributed to the cardioprotective role of 17β-estradiol, or estrogen, in younger women, effects that are lost in estrogen-deplete females and/or in older women post-menopause [17-20]. In parallel with the protective effects of low LDL cholesterol and prostacyclin, it is now also widely accepted that some of the cardioprotective effects of estrogen (E<sub>2</sub>) are also mediated through its ability to regulate expression and signalling by the protective prostacyclin/IP axis. For example, E<sub>2</sub> increases expression of COX<sub>1/2</sub> and PGIS [21], resulting in up to 6-fold elevations in systemic prostacyclin levels, while female IP<sup>-/-</sup>/LDLR<sup>-/-</sup> double null mice lose the atheroprotective effects of E<sub>2</sub> observed in LDLR<sup>-/-</sup> single knockout mice [22]. Moreover, E<sub>2</sub> can directly upregulate expression of the IP through a transcriptional mechanism involving direct binding of the estrogen receptor (ER)<sub>α</sub> to a highly conserved estrogen response element (ERE) within the PTGIR promoter [23].

Similar to the protective effects of estrogens in women, it is now also suggested that androgens may also confer certain cardioprotective effects in men although this is not without controversy [24-27]. Indeed, recent studies show a clinical correlation between low testosterone levels and risk/onset of CVD. For example, there is an increased incidence of CVD in patients where androgen levels are insufficient/deficient,

including in men with hypogonadism and in men undergoing androgen deprivation therapy (ADT) as part of their treatment for prostate cancer [28-30]. Consistent with this, a 5 year study in elderly men showed that high serum testosterone was associated with a decreased risk of cardiovascular incidents [31]. Testosterone, or its more active metabolite 5 $\alpha$ -dihydrotestosterone (DHT), mainly signals through the androgen receptor (AR), a member of the nuclear receptor family of steroid hormone receptors [32]. Androgen (testosterone/DHT)-binding to the AR induces a conformational change in the AR involving release of several heat shock proteins, AR-phosphorylation, homodimerisation and transcriptional activation of target genes with *cis*-acting androgen response elements (AREs) within their regulatory promoter regions [33]. The role of the AR in conferring protection against atherosclerosis was demonstrated in AR<sup>-/-</sup> null mice where double AR<sup>-/-</sup>/ApoE<sup>-/-</sup> null mice show an increased rate of atherosclerotic events compared to the single knockouts [34]. Furthermore, administration of testosterone reduced the rate of atherosclerosis in both ApoE<sup>-/-</sup> mice and AR<sup>-/-</sup>/ApoE<sup>-/-</sup> mice, suggesting that there may be androgen-independent as well as androgen-dependent mechanisms involved in this atheroprotection [34]. In addition to this, androgens may also influence expression of genes involved in cholesterol (CHO) metabolism, including in the co-ordinate upregulation of genes involved in both fatty acid and CHO synthesis [35]. Noteworthy, the observed androgen-mediated upregulation of genes involved in lipid/CHO metabolism does not occur through the classic direct AR-dependent mechanism, but rather occurs through a novel, indirect AR-independent mechanism of androgen action involving AR-induced activation of the aforementioned cholesterol-responsive SREBP and, in turn, leading to transcriptional upregulation of SREBP-SRE targeted genes [36, 37].

However, despite such convincing evidence supporting the role of androgens in cardioprotection in men, the underlying mechanism(s) whereby this occurs remain largely unknown. In view of the critical role of prostacyclin within the vasculature, including in mediating many of the atheroprotective effects of both reduced serum cholesterol and estrogen (E<sub>2</sub>), a compelling question arises regarding the possible influence of androgens on the prostacyclin-IP axis. Hence, focussing on the IP, the aim of the current study was to investigate whether the androgen dihydrotestosterone (DHT) regulates expression and function of the IP within the vasculature and to explore the mechanism(s) by which this regulation might occur. Herein, we uncovered a functional ARE located in the core promoter region of the PTGIR, lying within close proximity to the previously discovered cholesterol-responsive SRE [16]. Furthermore, it was established that DHT significantly increased IP expression in cultured vascular endothelial cells and in platelet-progenitor human erythroleukemic (HEL) cells which occurred through the direct binding of the AR to the ARE located within the core promoter. Moreover, it was discovered that in conditions of low cholesterol, DHT can lead to a further increase on IP/PTGIR expression through a co-ordinated mechanism involving binding of the AR and SREBP to the ARE and SRE, respectively, which lie in close proximity to each other within the core PTGIR promoter. Collectively, this study not only greatly advances understanding of the factors determining the transcriptional regulation of the PTGIR, but also helps to delineate the possible mechanisms whereby androgens may offer cardioprotection including in response to serum-cholesterol levels.

### 3. Materials and Methods

#### Materials

Dual Luciferase<sup>®</sup> assay system, pGL3Basic (pGL3B) and pRL-Thymidine Kinase (pRL-TK) were from Promega. The DMRIE-C<sup>®</sup>, RPMI 1640 media, L-glutamine, fetal bovine serum (FBS), Alexa Fluor 488-conjugated anti-rabbit IgG, Superscript reverse transcriptase and TRIzol were from Invitrogen Life Sciences. Dulbecco's Modified Eagle Medium (DMEM) and Endothelial Cell Growth Supplement/Heparin (ECGS/H) were from Lonza. Effectene<sup>®</sup> was from Qiagen. Low cholesterol serum was from Panbiotech. The Brilliant II Sybr Green QPCR kit and pCRE-luc were from Agilent. *Anti-AR* (sc-816X), *anti-SREBP1* (sc-8984X), goat *anti-rabbit* horseradish peroxidase (HRP; sc-2004), goat *anti-mouse* HRP (sc-2005) were from Santa Cruz Biotechnology. *Anti-HDJ2* was from Neomarkers. Medium 199, dextran-coated charcoal, actinomycin D (ActD), cycloheximide (CHX),  $\beta$ -estradiol (E<sub>2</sub>), dihydrotestosterone (DHT), ICI 182 780, hydroxyflutamide (HF) and bicalutamide (BIC) were from Sigma. Enzalutamide (ENZ) was from Selleck Biochem. All oligonucleotides were from Sigma-Genosys and *small interfering* (si)RNAs were synthesized by Eurofins Scientific.

#### Cell culture

Human erythroleukemic (HEL) 92.1.7 cells, obtained from American Type Culture Collection, were cultured in RPMI 1640, 10% fetal bovine serum (FBS). Human endothelial EA.hy926 cells, obtained from the Tissue Culture Facility at UNC Lineberger Comprehensive Cancer Centre, Chapel Hill, NC, were cultured in DMEM, 10% FBS. Primary (1<sup>°</sup>) human umbilical vein endothelial cells (HUVECs; Lonza), were cultured in M199 media supplemented with 0.4% v/v Endothelial Cell Growth Supplement/Heparin (ECGS/H; Lonza) and 20% FBS. For hormone studies, cells were cultured in media supplemented with 10% charcoal stripped-normal serum (CS-NS). The androgen receptor (AR) antagonists hydroxyflutamide (HF; 100 nM), bicalutamide (BIC; 50  $\mu$ M) and enzalutamide (ENZ; 10  $\mu$ M) were used at the previously recommended concentrations [38-40]. Where cholesterol levels were modified, cells were serum starved (0.1% FBS) overnight, then cultured in either 10 % CS-NS or 10% charcoal stripped-low cholesterol serum (CS-LCS) for 24 hr. All mammalian cells were grown at 37°C in a humid environment with 5% CO<sub>2</sub> and were confirmed mycoplasma free.

#### Quantitative Reverse Transcriptase-PCR analysis

Total RNA was isolated from  $\sim 5 \times 10^6$  HEL 92.1.7, EA.hy926 cells and 1<sup>°</sup> HUVECs using TRIzol reagent (Invitrogen). DNaseI treated total RNA (1  $\mu$ g/20  $\mu$ l reaction) was then converted into first strand (1<sup>°</sup>) cDNA using Superscript reverse transcriptase (Invitrogen). Quantitative real-time PCR (qRT-PCR) analysis was performed using the Brilliant II SYBR Green QPCR system as previously described [16] to amplify a 348 bp region of hIP mRNA (forward, 5'-GAAGGCACAGCGCACGGGA-3', Nu -57 to -37 of exon 1; reverse 5'-GGCGAAGGCGAAGGCATCGC-3', Nu 294 to 275 of exon 2), a 129 bp region of SCAP mRNA (forward, 5'-TGCTACCGTGGGGATGTCAC-3' Nu 3726 to 3746; reverse 5'-CAGGTCCTGCTGAATGGAGTAG-3', Nu 3834 to 3855) or, as a reference control, a 149 bp region of the human 18s rRNA gene (forward, 5'-AACCCGTTGAACCCCATTCG- 3', Nu +685 to +707; reverse, 5'-CGCTACTACCGATTGGATGG- 3', Nu +1176 to 1196). Levels of hIP and SCAP mRNA were normalised against 18s rRNA levels and relative mRNA expression levels were calculated using the 2<sup>- $\Delta\Delta$ Ct</sup> method [41]. Data is presented as mean changes in IP or SCAP mRNA expression relative to the levels in control, vehicle-treated cells, assigned a value of 1 (Relative expression  $\pm$  SEM, n=3, where 'n' refers to independent experiments and not replicates within the same experiment).

#### Luciferase-Based Genetic Reporter Plasmids

Recombinant pGL3B plasmids encoding the human prostacyclin receptor (hIP) promoter (PrmIP, nucleotides -2427 to -772 relative to the translational start codon, +1) and the 5' deletion fragments of PrmIP, denoted PrmIP1 through to PrmIP7, along with pGL3B:PrmIP2<sup>ERE\*</sup> and pGL3B:PrmIP6<sup>SRE\*</sup> were

previously described [16, 23, 42]. The pPSA and pMMTV luciferase-based gene reporter plasmids encoding the promoter regions of the prostate specific antigen (PSA) and mouse mammary tumour virus (MMTV) genes, respectively, [43] were kindly provided by Prof Roland Schüle, University Freiberg Medical Centre, Germany. QuickChange™ site directed mutagenesis (SDM) was used to mutate the putative ARE (-984) from ggaGaaCagt to ggaTaaTagt using the template pGL3B:PrmIP2 or pGL3B:PrmIP6 and the complementary primers: forward 5'-AGGGGGCCCTCTGGATAATAGTGAAGGGAGGGCGGG-3', reverse 5'-CCCGCCCTCCCTCCCTCACTATTATCCAGAGGGCCCCCT-3' to generate the plasmids pGL3B:PrmIP2<sup>ARE(-984)\*</sup> and pGL3B:PrmIP6<sup>ARE(-984)\*</sup>. Similarly, the SRE (-937) was mutated from gtgAgca to gtgGgca using the template pGL3B:PrmIP6<sup>ARE(-984)\*</sup> and the complementary primers: forward 5'-GAAATGAAAAGCTGGGGTGGGCAAGGCAAGCTGAGGAGG-3', reverse 5'-CCTCCTCAGCTTGCCTGCCTGCCACCCCAGCTTTTTTCATTTC-3' to generate pGL3B:PrmIP6<sup>ARE(-984)\*SRE(-937)\*</sup>. All plasmids were validated by DNA sequence analysis.

### Luciferase-based genetic reporter assays

HEL and EA.hy926 cells were serum starved overnight (0.1% FBS) and cultured in 10% CS-NS or 10% CS-LCS for 24 hr prior to co-transfection with various pGL3B-recombinant plasmids (2 µg), encoding firefly luciferase, along with pRL-TK (200 ng, renilla luciferase) using DMRIE-C® [16]. 1°HUVECs were cultured in 10% CS-NS and co-transfected with the pGL3B-recombinant plasmids (firefly luciferase), along with pRL-TK (renilla luciferase) as previously described using Effectene® [16]. For hormone studies, cells were incubated with either 10 nM DHT, 10 nM E<sub>2</sub> or the drug vehicle (0.01% EtOH) for 24 hr. Cells were harvested 48 hr post transfection as per the Dual Luciferase® assay system (Promega) and firefly and renilla luciferase activities measured. Relative luciferase units were calculated and expressed as a ratio of firefly to renilla luciferase (relative luciferase units, RLUs; n=3, where 'n' refers to independent experiments and not replicates within the same experiment) [16].

To investigate changes in agonist-induced cAMP generation, HEL and EA.hy926 cells were co-transfected with the cAMP-responsive luciferase reporter plasmid pCRE-Luc (1 µg, Stratagene) along with pRL-TK (50 ng). Some 48 hr post transfection, cells were incubated with either 10 nM DHT, 10 nM E<sub>2</sub>, 10 nM DHT plus 100 nM HF, 10 nM E<sub>2</sub> plus 100 nM ICI or the drug vehicle (0.01% EtOH) for 24 hr. Cells were then pre-incubated with the phosphodiesterase inhibitor IBMX (100 µM) for 30 min prior to stimulation with 1 µM cicaprost or vehicle (0.01% EtOH) at 37 °C for 3 hr. Firefly and renilla luciferase activities were assayed using the Dual Luciferase® Assay System and cAMP levels generated in vehicle- or cicaprost-treated cells were expressed as a ratio (RLUs) or as fold-inductions in cAMP accumulation (n=3, where 'n' refers to independent experiments and not replicates within the same experiment) [23].

### Cell Migration Assays

To monitor changes in EA.hy926 cell migration, cells were seeded onto 12 well plates such that 90% confluency was achieved after 24 hr. Thereafter, cells were cultured in serum-free media and preincubated with either DHT (10 nM) or drug vehicle (0.01% EtOH) for 24 hr. Each well was washed with serum-free media (x2) before scoring from top to bottom with a 200 µl pipette tip. Loose debris and cells were washed away with serum-free media and replaced with 500 µl of serum-free media. Cells were preincubated with either the IP antagonist RO1138452 (10 µM) or vehicle (0.01% PBS), prior to stimulating with cicaprost (1 µM) or vehicle (0.01% EtOH). Cells were imaged immediately after treatment (0 hr) or following 8 hr incubations at 37 °C. Images were captured with a Nikon TMS inverted microscope with Matrox Intelicam software (version 2.07) and analysed using the TScratch software (version 1.0). Cicaprost-induced EC migration was expressed as a percentage of basal cell migration, determined in the presence of the drug-vehicle. All stimulations were carried out in duplicate, where 4 independent experiments were carried out (n=4, where 'n' refers to independent experiments and not replicates within the same experiment).

### **Immunofluorescence Microscopy**

To examine human (h)IP expression, 1°HUVECs were serum starved overnight (0.5% FBS) and cultured in 20% CS-NS or 20% CS-LCS prior to seeding on to poly-L-lysine coated coverslips in 6 well plates [16]. Cells were incubated for 24 hr with either 10 nM DHT, 10 nM E<sub>2</sub>, 10 nM DHT plus 100 nM HF, 10 nM DHT plus 50 μM BIC, 10 nM DHT plus 10 μM ENZ or vehicle (0.01% EtOH). Thereafter, cells were fixed with 3.7% paraformaldehyde (pH 7.4) for 15 min (room temperature, RT) and washed with 1X PBS. Cells were then permeabilised using 0.2% Triton-PBS for 10 min on ice and washed in 1X TBS (10 mM Tris-HCl, 100 mM NaCl, pH 7.4). For immunolabelling, non-specific sites were blocked using 5% milk dissolved in 1X TBS, prior to incubation overnight at 4°C with the affinity-purified *anti*-hIP antibody (1 in 500, 5% milk-TBS). The hIP antibody, directed to intracellular loop 2 (IC<sub>2</sub>) of the human IP, has been previously described [23]. To demonstrate antibody specificity, the *anti*-hIP sera was pre-incubated with an antigenic IC<sub>2</sub> peptide (10 μg/ml) for 1 hr (RT) prior to overnight incubation of the cells [23]. Following incubation with the primary antibody, cells were washed in 1X TBS, blocked for a further 30 min in 5% milk dissolved in 1X TBS and incubated with AlexaFluor 488 *anti*-rabbit (1 in 2000, 5% milk-TBS) for 1 hr (RT). Cells were counterstained using 4'-6-diamidino-2-phenylindole (DAPI, 1 μg/ml in H<sub>2</sub>O) and coverslips were mounted in Mowiol mounting medium. Image analysis was carried out using a Zeiss Axioplan 2 microscope (63 x magnification) and Axioplan version 4.4 imaging software. Images are representative of 3 independent experiments, where at least 9 independent images were captured for quantitation. Quantitation of corrected total cell fluorescence (CTCF) was carried out using the image analysis software ImageJ and the formula: CTCF=Integrated density – (Area of cell x Mean background fluorescence).

### **Small interfering (si) RNA mediated disruption of the AR and SREBP1**

1°HUVECs were serum starved overnight (0.5% FBS) and cultured in 20% CS-NS or 20% CS-LCS for 24 hr. Cells were then transiently transfected with *si*RNA specifically targeting either the AR (*si*RNA<sub>AR</sub>, 5'-GGA ACU CGA UCG UAU CAU U-3'), SREBP1 (*si*RNA<sub>SREBP1</sub>, 5'-GAG AGA AGC GCA CAG CCC A-3') or a non-specific scrambled control *si*RNA (*si*RNA<sub>CONTROL</sub>, 5'-UUC UCC GAA CGU GUC ACG U-3') using Dharmafect 4, where a final concentration of 30 nM *si*RNA was used. All *si*RNA data was independently validated with the following additional *si*RNA sequences directed to the AR and SREBP1: *si*RNA<sub>AR#2</sub>, 5'-GCU GAA GAA ACU UGG UAA U-3'; *si*RNA<sub>SREBP1#2</sub>, 5'-GCA AGG CCA UCG ACU ACA U-3'. Transfected cells were seeded at a density of 1.5 x 10<sup>6</sup> cells/100 mm diameter dish and harvested 96 hr post-transfection. For immunofluorescence analysis of hIP expression, transfected cells were initially seeded at a density of 1.5 x 10<sup>6</sup> cells/100 mm diameter dish for 48 hr before plating on to coverslips. *si*RNA mediated disruption of the AR and SREBP1 was confirmed by immunoblot analysis with *anti*-AR or *anti*-SREBP1 respectively. To detect AR or SREBP1 proteins, whole cell extracts (20 μg per lane) were resolved by SDS-PAGE on 8 -10% acrylamide gels and proteins were transferred to polyvinylidene difluoride (PVDF) membranes, as per standard methodology. Membranes were blocked in 5% milk powder dissolved in 1X TBS for 1 hr at room temperature and incubated overnight with either *anti*-AR or *anti*-SREBP1 at 4 °C. Membranes were washed and screened with goat *anti*-rabbit horseradish peroxidase, followed by chemiluminescence detection. As a reference for uniform protein loading, all blots were rescreened with an *anti*-HDJ2 followed by goat *anti*-mouse HRP and detection by chemiluminescence. Blots are representative of 3 independent experiments.

### **Chromatin immunoprecipitation (ChIP) assays**

Chromatin immunoprecipitation (ChIP) assays were performed in EA.hy926 cells as previously described [16]. Briefly, ~1X10<sup>8</sup> cells were cultured in DMEM supplemented with either 10% CS-NS or 10% CS-LCS for 24 hr, prior to incubation with 10 nM DHT or vehicle (0.01% EtOH). Chromatin was cross-linked by adding formaldehyde (1%) dropwise to cells with gentle agitation, followed by addition of 3 M glycine. Cells were lysed to release chromatin and sheared by sonication to generate 350-1000 bp fragments.

Chromatin was pre-cleared by incubating with normal rabbit IgG overnight on a rotisserie, followed by incubation with 250 µl salmon sperm DNA-protein A agarose beads (Millipore) overnight, with rotation. Input chromatin was taken after pre-clearing and before immunoprecipitation and kept at -20 °C for later use. For immunoprecipitation, pre-cleared chromatin was incubated with *anti-AR* (10 µg), *anti-SREBP1* (10 µg), normal rabbit IgG (10 µg) or in the absence of primary antibody overnight at 4 °C. Complexes were eluted from the salmon sperm DNA-protein A agarose beads and incubated with RNase A at 65 °C overnight, followed by incubation with Proteinase K at 45 °C for 7 hours. Complexes were precipitated and resuspended in H<sub>2</sub>O. PCR analysis was carried out by typically using 1:5 dilutions of immunoprecipitated template or 1:20 dilutions of Input chromatin. Independent primer sets 1 and 2 used for amplification of the test (PTGIR) region and primers used for the control (TBXA2R) region were as follows:

1. Test (PTGIR; 5' Primer 1): 5' GACGGGGAGTGGGGAGTG 3' (Nt -1019 to -1001)
2. Test (PTGIR; 3' Primer 1): 5' CTCTCGCTGCCTGTGTCG 3' (Nt -859 to -841)
3. Test (PTGIR; 5' Primer 2): 5' GAGAGGTACCACCCTGAGACAGCCCAGG 3' (Nt -1271 to -1243)
4. Test (PTGIR; 3' Primer 2): 5' CTCTCAAGCTTCTCTCTCCAGTCTTGCCAGGCTC 3' (Nt -807 to -774)
5. Control (TBXA2R; 5' Primer): 5' CATGCAATTCCTGTCACTGC 3' (Nt -7718 to -7698)
6. Control (TBXA2R; 3' Primer): 5' GTGAGCTAGGAAGACATCTTG 3' (Nt -7631 to -7610)

For quantification of PCR products obtained from ChIP experiments, the relative density (arbitrary units) of amplicons generated due to AR and SREBP1 binding to PrmIP was measured using the GeneTools software, where the Input DNA was calibrated to 100 and the no 1° AB was calibrated to 0. AR and SREBP1 binding is expressed as a % of input loaded (n=3, where 'n' represents 3 independent pulldowns, and where each pulldown was analysed by PCR twice).

### Statistical Analysis

Statistical analysis was carried out using the two-tailed Student's unpaired *t*-test, one or two-way ANOVA followed by post-hoc Bonferroni's or Dunnett's multiple comparison *t*-tests using GraphPad Prism version 6.0 or IBM SPSS version 20. All values are expressed as mean ± standard error of the mean (SEM). *P* values ≤ 0.05 were considered to indicate statistically significant differences; \**P* ≤ 0.05, \*\**P* ≤ 0.01, \*\*\**P* ≤ 0.001, \*\*\*\**P* ≤ 0.0001.

## 4. Results

### 4.1 Effects of the androgen DHT on regulating PTGIR expression

As stated, the cardioprotective effects of prostacyclin and of the female hormone estrogen ( $E_2$ ) are well documented [21]. Indeed expression of the prostacyclin receptor (IP) gene, the PTGIR, can be directly regulated by  $E_2$  which occurs through a transcriptional mechanism involving direct binding of the estrogen receptor ( $ER$ ) $\alpha$  to a conserved estrogen response element (ERE) within the promoter region of the PTGIR [23]. While typically men present with CVD some 10 years earlier than women, emerging evidence suggests that like  $E_2$ , androgens including testosterone or its active metabolite dihydrotestosterone (DHT) may also offer certain cardioprotection in men. Hence, the aim of this study was to explore whether androgens, namely DHT, can regulate the PTGIR, where the megakaryoblastic HEL 92.1.7 served as a model platelet progenitor, and EA.hy926 cells and primary ( $1^\circ$ ) human umbilical vein endothelial cells (HUVECs) served as model vascular endothelial cell lines, respectively.

Initially, real-time quantitative reverse transcriptase (qRT)-PCR was used to investigate the effects of DHT on human (h) IP mRNA expression in HEL 92.1.7 and EA.hy926 cells, where incubation with  $E_2$  served as a positive reference control. Consistent with previous data [23],  $E_2$  yielded significant increases in hIP mRNA expression, an effect abrogated by the  $E_2$  antagonist ICI 182,780 in both cell lines (Figure 1A & 1B). In HEL cells, incubation with DHT (10 nM) resulted in 3.9-fold increases in hIP mRNA expression (Figure 1A), while the AR antagonist hydroxyflutamide (HF) completely abolished the DHT-induced increase in hIP expression (Figure 1A). In concentration response studies, 10 nM DHT was found to be the optimal concentration required to bring about the induction in hIP mRNA expression in both HEL and EA.hy926 cells (Supplemental Figure 1A & 1B). Neither the ER antagonist ICI 182,780 nor the AR antagonist HF alone had any effect on hIP mRNA expression (Figure 1A). Furthermore, preincubation with the transcriptional inhibitor actinomycin D (ActD), but not with the translational inhibitor cycloheximide (CHX), abrogated the DHT-induced upregulation of hIP mRNA expression (Figure 1C), confirming that DHT regulates the PTGIR at the transcriptional level. Similar to HEL cells, DHT increased hIP expression in EA.hy926 cells (Figure 1B, 5.3-fold), an effect that was abolished by the AR antagonist HF (Figure 1B) and by ActD (Figure 1D).

Previous studies have characterized the human IP promoter, herein denoted the PrmIP, as nucleotides spanning -2449 to -772, relative to the translational start codon (+1) [42] within the PTGIR, where the core promoter region was localised to the subfragment PrmIP6 (-1042 to -772 nucleotides, relative to +1) [42]. Hence, the effect of DHT on PrmIP and PrmIP6-directed promoter activity was initially investigated in HEL and EA.hy926 cells through luciferase-based gene reporter assays. In response to DHT stimulation, dose-dependent increases in PrmIP-directed gene expression (Figure 1E, 1.71-fold,  $P < 0.00139$ ; 10 nM) and in PrmIP6-directed gene expression (Figure 1F, 1.78-fold,  $P < 0.0057$ ; 10 nM) were observed in HEL cells and in EA.hy926 cells (Supplemental Figure 1C). Furthermore, the selective AR antagonists HF, bicalutamide (BIC) and enzalutamide (ENZ) abolished the DHT induced increase in PrmIP6-directed gene expression (Figure 1G,  $P < 0.001$ ; data not shown for PrmIP). Collectively, these data confirm that DHT upregulates hIP mRNA expression and PrmIP-directed gene expression through an AR-dependent transcriptional mechanism.

### 4.2 Effect of DHT on hIP expression and function

As stated, the hIP is primarily coupled to Gs-mediated adenylyl cyclase activation leading to increases in cellular cAMP levels [44]. To establish whether DHT-mediated increases of PTGIR expression also lead to functional changes in hIP expression, the effect of DHT on cAMP generation was investigated in HEL and EA.hy926 cells following stimulation of the IP with its selective agonist cicaprost. Consistent with previous data [23],  $E_2$  significantly increased cicaprost-induced cAMP generation in HEL cells (Figure 2A & 2B) and in EA.hy926 cells (Figure 2C & 2D). Similarly, DHT also resulted in substantial increases in cicaprost-induced cAMP accumulation in both cell types (HEL, Figure 2A & 2B, 4.7-fold,  $P < 0.0001$ ; EA.hy926,

Figure 2C & 2D, 4.6- fold,  $P < 0.0001$ ), an effect that was abrogated by the AR antagonist HF (HEL, Figure 2A & 2B; EAhy926, Figure 2C & 2D).

To establish whether such DHT-induced increases in hIP expression in endothelial cells correlates with downstream functional changes in hIP-mediated cellular responses, the effect of DHT on hIP-mediated migration of EA.hy926 cells was investigated (Figure 2E & 2F). Consistent with previous studies [45], the IP agonist cicaprost (1  $\mu$ M), but not its antagonist RO1138452 (10  $\mu$ M), induced an increase in EA.hy926 cell migration. Furthermore, pre-incubation of EA.hy926 cells for 24 hr with DHT (10 nM) resulted in a significant increase in cicaprost-induced EA.hy926 cell migration, an effect that was inhibited by the IP antagonist RO1138452, confirming specificity and that the DHT-induced increase in hIP expression results in downstream functional changes, including enhanced EC migration (Figure 2E & 2F).

To confirm that DHT-induced increases in hIP expression can occur more widely within the vasculature, the effect of DHT on hIP expression was investigated in 1° human umbilical vein endothelial cells (HUVECs). Briefly, qRT-PCR analysis confirmed DHT-induced increases in hIP mRNA expression (Figure 3A), an effect that was abolished by the AR antagonist HF (Figure 3A) and the transcriptional inhibitor ActD, but not by CHX (Figure 3B). Subsequent to this, immunofluorescence microscopy was used to confirm changes in hIP expression in response to DHT, where 1°HUVECs were stained with an affinity purified antibody directed to intracellular loop 2 (IC<sub>2</sub>) of the hIP [23]. DHT (10 nM; 24 hr) increased hIP expression compared to vehicle-treated cells (Figure 3C & 3D). Furthermore, the AR antagonists HF, BIC and ENZ completely abolished the DHT-induced upregulation of hIP expression in HUVECs (Figure 3C & 3D). The specificity of the *anti*-hIP antibody was confirmed by peptide competition, where pre-incubation of the hIP antibody with an antigenic IC<sub>2</sub> peptide completely blocked detection of the hIP (Figure 3C). Collectively, these data establish that DHT upregulates hIP expression in platelet progenitor and endothelial cell lineages of the vasculature and occurs through an AR-dependent mechanism leading to enhanced hIP expression and signalling.

### 4.3 Identification of the Androgen responsive region (ARR) within the PrmIP

Having established that hIP expression is regulated by an AR-dependent transcriptional mechanism, 5' deletional analyses of PrmIP combined with luciferase-based genetic reporter assays was used to localise the androgen responsive regions (ARRs) in HEL (Figure 4A), EA.hy926 (Figure 4B) cells and 1°HUVECs (Figure 4C). Consistent with previous findings, the core promoter region, defined as the minimum region required for basal transcription, was localised to the PrmIP6 subfragment in all 3 cell types and corresponds to the region between nucleotides -1042 to -917 (Figure 4A – 4C). In HEL cells, incubation with DHT resulted in similar 1.5 – 2 -fold increases in PrmIP- and PrmIP1 – PrmIP6- directed luciferase expression ( $P < 0.001$ ; Figure 4A & Supplemental Figure 2A), an effect which was lost in the smaller PrmIP7 subfragment. Specifically, deletion of nucleotides -1042 to -917 resulted in loss of the DHT-induced increases in PrmIP-directed gene expression, confirming the presence of an ARR within PrmIP6 and larger subfragments, but not within the smaller PrmIP7 subfragment. Likewise, in EA.hy926 cells and 1°HUVECs, the ARR was localised to within PrmIP6, where DHT led to 1.5 – 2 -fold increases in PrmIP6-directed gene expression (EA.hy926,  $P < 0.0001$ , Figure 4B & Supplemental Figure 2B; HUVECs,  $P < 0.0001$ , Figure 4C & Supplemental Figure 2C). In contrast to the megakaryoblastic HEL and primary vascular cells (1°HUVECs), the PrmIP and PrmIP1 subfragments failed to show a significant response to DHT in the endothelial EA.hy926 cell line, suggesting the presence of a cellular-specific repressor region between PrmIP1 and PrmIP2. This region was not investigated further within this study.

Thereafter, bioinformatic analysis, using the Genomatix software suite [46], identified a perfect ARE consensus *cis*-acting element with the sequence 5'-TGTTCT-3' within PrmIP, and which is evolutionary conserved and specifically localised within the PrmIP6 subfragment at 5' nucleotide at -984. As stated, previous studies have also identified a functional E<sub>2</sub>-responsive ERE within the PrmIP, specifically localised upstream from the core promoter at -1676 in PrmIP2 [23]. Hence, the effect of disrupting the putative ARE in both the E<sub>2</sub>-responsive PrmIP2 (Figure 5A – 5C) and the androgen-responsive PrmIP6 (Figure 5D – 5F)

subfragments were investigated through site-directed mutagenesis and luciferase-based gene reporter assays. Mutating the ARE reduced the DHT-induced increase in both PrmIP2- and PrmIP6-directed gene expression in HEL (Figure 5A & 5D,  $P < 0.0001$ ), EA.hy926 (Figure 5B & 5E,  $P < 0.0001$ ) cells and in HUVECs (Figure 5C & 5F,  $P < 0.0001$ ). While mutating the ERE within PrmIP2 had no significant effect on the DHT-response in all 3 cell lines (Figure 5A – 5C), as expected it abolished the E<sub>2</sub> response consistent with previous studies [23]. Moreover, mutation of the ARE had no effect on E<sub>2</sub>-induced increases PrmIP2-directed gene expression (Supplemental Figure 3) demonstrating that E<sub>2</sub> and DHT function independently of each other to regulate PrmIP-induced hIP expression in these model cells lines.

As stated, in addition to an ERE, the PrmIP also contains a cholesterol-responsive sterol response element (SRE) that is localised to the core promoter region within PrmIP6 [16] and, therefore, this SRE lies adjacent to the putative ARE identified herein. Hence, in view of the proximity of the functional SRE (-937) to the putative ARE (-984) combined with the fact that androgens can also regulate target gene expression through an AR-mechanism that is dependent on its regulation of SREBP/SRE- mediated transcriptional regulation [35], the possible role of the SRE within the PrmIP in mediating the DHT-induced transcriptional responses was also investigated. Disrupting the SRE had no significant effect on the DHT-induced increases in PrmIP6-directed reporter gene expression in HEL cells (Figure 5D), EA.hy926 cells (Figure 5E) and HUVECs (Figure 5F). Together, these data confirm that PrmIP contains an ARR localised to the core promoter region whereby the PrmIP6 subfragment contains the functional ARE. Furthermore, this novel ARE acts independently of the E<sub>2</sub>-responsive ERE and CHO-responsive SRE found at upstream and adjacent regions, respectively, within the PrmIP.

#### **4.4 Role of low-cholesterol and SREBP1 in the androgen regulation of PTGIR**

While these latter studies suggest that the cholesterol (CHO)-responsive SRE had no effect on DHT-induced increases in PrmIP6-directed gene expression when cells were cultured in normal serum conditions (Figure 5D-5F), they did not exclude the possibility that the SREBP-SRE axis may contribute to the DHT-AR response in low/reduced serum CHO conditions. Previous studies have shown that low serum CHO regulates the PTGIR through binding of SREBP1 to the functional SRE contained within PrmIP6 [16], while other studies show that SREBP1 can contribute to androgen/DHT-induced gene expression through an indirect AR- mechanism also in conditions of low serum CHO [35]. Therefore, to investigate whether DHT might also regulate hIP expression through the functional SRE in low CHO conditions, HEL (Figure 6A– 6C) and EA.hy926 (Figure 6D – 6F) cells were cultured in either normal serum or low CHO serum, prior to incubation with DHT. Consistent with previous data, genetic reporter analysis confirmed the presence of the cholesterol-responsive region within the PrmIP6 (-1042 to -772, Figure 6) while mutation of the SRE resulted in a significant loss of PrmIP6-directed gene expression in both HEL ( $P < 0.0001$ , Figure 6A) and EA.hy926 (Figure 6D,  $P < 0.0001$ ) cells in the presence of low CHO serum [16]. As found previously, in normal serum CHO conditions, the DHT-induced response was abrogated following mutation of the ARE within PrmIP6 (HEL, Figure 6B,  $P < 0.0001$ ; EA.hy926, Figure 6E,  $P < 0.0001$ ), but mutation of the SRE had no effect (Figure 6B & 6E). However and in direct contrast, disrupting either the functional ARE and/or the SRE each resulted in significant losses in DHT-induced PrmIP6-directed gene expression in both HEL (Figure 6C,  $P < 0.0001$ ) and EA.hy926 (Figure 6F,  $P < 0.0001$ ) cells cultured under low CHO conditions.

In addition to the direct AR-mediated mechanism, androgens can also enhance target gene expression in conditions of low serum CHO through an established mechanism involving DHT-AR induced upregulation of the CHO-sensor SREBP cleavage activating protein (SCAP) leading, in turn, to enhanced site-1 protease (S1P)- and S2P-proteolytic processing and maturation of SREBP facilitating subsequent binding of the cleaved transcriptionally active basic helix-loop-helix leucine zipper (bHLH-LZ) domain of SREBP to SRE *cis*-elements within target promoters [37]. Hence, the effect of DHT on SCAP mRNA expression was investigated in cells cultured in normal and low CHO conditions (Figure 7). In normal serum, DHT had no effect on SCAP mRNA expression relative to the vehicle in either megakaryoblastic HEL or vascular endothelial EA.hy926 cells while in cells cultured in low CHO, DHT resulted in a 2.4-fold increase

in SCAP mRNA expression in HEL cells and a 3.5 –fold increase in EA.hy926 cells, effects that were inhibited by the AR-antagonists hydroxyflutamide, bicalutamide and enzalutamide (Figure 7A & 7B). Furthermore, and consistent with this and with previous studies [16, 35-37], both reduced serum conditions and DHT led to increased processing of SREBP1 (data not shown).

Thereafter, the relative roles of the AR and SREBP1 in the DHT-induced upregulation of hIP expression was investigated through immunofluorescence microscopy in 1° HUVECs cultured in normal serum and in low CHO serum where *silencing* (*si*) RNA sequences were used to specifically down-regulate AR (*siRNA<sub>AR</sub>*) and SREBP1 (*siRNA<sub>SREBP1</sub>*) expression (Figure 8). Initially, effective *siRNA*-mediated disruption of the AR and SREBP1 was confirmed by immunoblotting, where each *siRNA* resulted in near complete knockdown of AR and SREBP1 expression (Figure 8D). In normal serum, DHT significantly increased hIP expression in 1°HUVECs (Figure 8Ai; Figure 8C,  $P<0.0001$ ) while *siRNA<sub>AR</sub>*-disruption of the AR abolished this DHT-mediated upregulation (Figure 8Aiii; Figure 8C,  $P<0.0001$ ). In low CHO conditions, DHT further enhanced hIP expression relative to its effect on hIP expression in cells cultured in normal serum (Figure 8Bi, Figure 8C,  $P<0.0001$ ). However, disruption of either the AR (*siRNA<sub>AR</sub>*, Figure 8Biii; Figure 8C,  $P<0.0001$ ) or SREBP1 (*siRNA<sub>SREBP1</sub>*, Figure 8Biv; Figure 8C,  $P<0.0001$ ) significantly abrogated the DHT-induced enhancement of hIP expression, while the scrambled control *siRNA* had no effect (*siRNA<sub>CONTROL</sub>*, Figure 8Bii; Figure 8C).

Hence, taken together, these data suggest a role for the functional SRE in the DHT-induced upregulation of PrmIP-directed gene expression in 1° HUVECs cultured under low CHO conditions, whereby DHT increases SCAP expression and, in turn, leads to SREBP1-mediated increases in hIP expression.

#### 4.5 Confirmation of binding of the AR to PrmIP

To investigate whether the AR or SREBP1 can directly bind *in vivo* to chromatin surrounding the core promoter region of PrmIP in response to DHT, chromatin immunoprecipitation (ChIP) analysis was performed on chromatin extracted from EA.hy926 cells cultured in either normal serum (NS) or low CHO serum (LCS) prior to incubation with DHT or the drug-vehicle. As expected, PCR amplification of the PrmIP test region (e.g nucleotides -1019 to -841 of the PTGIR gene) and non-specific control region (nucleotides -7718 to -7610 of the TBXA2R gene) produced amplicons from the input chromatin extracted from EA.hy926 cells incubated with either the drug vehicle or with DHT (Figure 9A & 9B). Furthermore, and more specifically, PCR amplification and densitometric analysis confirmed that PCR amplicons were generated from the *anti-AR* immunoprecipitates for the test PrmIP region (Figure 9A, 9C & Supplemental Figure 4A & 4B) from cells pre-incubated with DHT but not from cells pre-incubated with the drug vehicle or from the corresponding minus antibody (-AB) or normal *anti-rabbit IgG* control immunoprecipitates (Figure 9A, 9C & Supplemental Figure 4A & 4B). For the *anti-SREBP1* immunoprecipitates, ChIP analysis confirmed that there was an increase in SREBP1 binding to chromatin surrounding the PrmIP core region in cells cultured in low CHO serum compared to normal serum (Figure 9A, 9C & Supplemental Figure 4A & 4B). Additionally, in low CHO serum, co-incubation with DHT resulted in further increases in SREBP1 binding to PrmIP relative to the drug vehicle (Figure 9C & Supplemental Figure 4;  $P<0.05$ ). No amplicons were generated for the control TBXA2R region following either *anti-AR*- or *anti-SREBP1*- ChIP pull-down, and regardless of serum condition or DHT/vehicle treatment (Figure 9B & Supplemental 4C & 4D),

Taken together, the data presented in this study establishes that DHT upregulates hIP/PTGIR expression through direct binding of the AR to an ARE within the PrmIP in model megakaryoblastic and endothelial cell lineages of the vasculature. The androgen-induced effects are independent of E<sub>2</sub>-mediated increases in hIP expression, with no involvement from the previously identified functional ERE. The SREBP1/SRE-axis does not influence androgen-induced upregulation of hIP expression under normal serum conditions. However, in conditions of low serum cholesterol, DHT can also lead to enhanced SREBP1 binding to the functional SRE within the PrmIP, further increasing hIP expression.

## 5. Discussion

Cardiovascular diseases (CVDs) are one of the leading causes of morbidity and premature mortality in the developed world [47, 48]. While the role of testosterone and other androgens in CVD risk in men is controversial [49, 50], recent clinical, epidemiological, cellular and animal studies have demonstrated that similar to the protective effects of E<sub>2</sub> in women, androgens can also have positive effects on the vasculature [25, 31, 34, 51, 52]. This is exemplified by the increased incidence of CV risk factors in men with hypogonadism or undergoing androgen deprivation therapy (ADT) as part of their treatment regimen for prostate cancer [28-30]. Mechanistically, androgens have been implicated in several cardioprotective processes including in preventing vascular remodelling and promoting re-endothelialisation, where reduced proliferation of vascular smooth muscle cells and increased growth of endothelial cells is observed in response to DHT [53]. Furthermore, orchietomized male rabbits raised on a high-cholesterol diet and treated with testosterone have reduced atherosclerotic plaque lesions compared to the untreated animals [54]. Interestingly, male rabbits treated with E<sub>2</sub> and female rabbits treated with testosterone showed no reduction in plaque formation, further indicating gender-specific cardioprotection by androgens and estrogens [54].

As stated, the COX metabolite prostacyclin is a central mediator and regulator of haemostasis within the vasculature [4]. Clinically, the importance of prostacyclin within the vasculature was highlighted by the withdrawal of certain selective COX2 inhibitors (COXIBs), where it was proposed that COX2 inhibition led to an imbalance in 'protective' prostacyclin synthesis without affecting thromboxane synthesis, a prostanoid involved in platelet aggregation and vasoconstriction [55]. This 'imbalance theory', although remaining somewhat controversial [56], is also supported by work in mouse model systems, where IP<sup>-/-</sup> mice exhibit several pro-thrombotic propensities while also losing the cardioprotection afforded by ischemic preconditioning (IPC) [57, 58]. Hence, understanding the factors that regulate prostacyclin signalling in the vasculature is of great physiological importance. Previous studies have demonstrated that estrogen (E<sub>2</sub>) directly regulates the PTGIR through an ER $\alpha$ -dependent transcriptional mechanism, where it was proposed that this upregulation of IP expression may account for some of the cardioprotective effects of E<sub>2</sub> [23]. Likewise, low-serum cholesterol increases COX2 expression and prostacyclin production in human endothelial cells [15]. Through more recent studies, it was also established that low-serum cholesterol enhances expression of the PTGIR through a transcriptional mechanism involving binding of the SREBP1-master regulator to an SRE *cis*-acting element within the core promoter/PrmIP [16]. Several lines of evidence now support a role for androgens in regulating the COX/prostacyclin axis [31, 55, 56, 57]. Exogenous testosterone administration partially rescues castration-associated decreases in both COX1 and COX2 mRNA expression in rat epididymis [59]. COX2 expression is upregulated in response to DHT in periovarian granulosa cells, where androgens were found to directly regulate the COX2 gene through an AR-dependent mechanism [60]. Within the vasculature, DHT increases COX2 expression in human coronary artery smooth muscle cells and, while not measured directly, that study suggested that DHT might lead to increased prostacyclin levels [61]. Consistent with that suggestion, testosterone leads to an enhanced vasodilatory response in diabetic rabbits compared with control animals and occurs, in part, due to increased COX2-derived prostacyclin synthesis [62].

The finding that both the female hormone estrogen and reduced serum cholesterol can regulate expression of the PTGIR within the vasculature prompted us to speculate about the possible influence of androgens such as testosterone or its more active metabolite DHT on IP expression. Hence, the over-arching goal of the current study was to investigate whether androgens might also regulate expression of the PTGIR within model platelet progenitor, megakaryoblastic and vascular endothelial cell lineages. It was established that DHT is indeed a *bone fide* regulator of the PTGIR and propose that this increased expression of the prostacyclin-IP axes might account for some of the protective effects of androgens within the vasculature. Specifically, DHT increased IP mRNA expression, IP-induced signalling and EC migration, and increased PrmIP-directed gene expression in all of the model cell lines used, where the androgen responsive region (ARR) was localised to the 'core' promoter region and found to involve AR binding to an ARE half-site (-984) located within the core PrmIP. While the ARR was localised to PrmIP6 in both megakaryoblastic and

vascular endothelial model cell lines, an additional upstream repressor region (nucleotides -1783 to -1703) was identified in the vascular endothelial cell line EA.hy926 not seen in either HEL 92.1.7 cells or in 1° HUVECs. Typically, transcriptional activation of target genes by the AR involves recruitment and release of a network of co-activators and co-repressors [63]. It is possible that binding of a *trans*-acting repressor within this region is blocking AR binding to PrmIP. While this region was not investigated in detail within the realms of this study and the identity of the *trans*-acting repressor factor(s) is unknown, it is the subject of ongoing investigations. In addition, in the current study, a combined role for low-cholesterol and DHT in regulating the PTGIR was identified, whereby DHT was found to enhance SREBP1 binding to the PrmIP and, thereby, increase IP expression. To our knowledge, this is the first demonstration that androgens can regulate the PTGIR within the vasculature and show that this occurs through both a classical AR-dependent mechanism and through a SREBP1-mediated pathway.

Androgens can have direct, fast acting effects on the vasculature [64], where the AR can mediate induction of signalling cascades by regulating intracellular Ca<sup>2+</sup> [65]. Moreover, the vasodilatory effects of androgens have been proposed to be mediated by ion channel modulation in the smooth muscle cells, sidestepping classical nuclear receptor action by the AR [66]. However, although some studies have elicited that protection within the vasculature is due to non-genomic effects [67], others have demonstrated slower transcriptional effects mediated through the AR [68]. Expression of the AR has been found in most cells of the vasculature, including in platelets and endothelial cells [69]. Human endothelial cells incubated with testosterone or its active metabolite DHT were found to increase levels of endothelial nitric oxide synthase (eNOS) through both AR-dependent and AR-independent pathways [70], indicating that cardioprotection by androgens may involve several different transcriptional and non-transcriptional mechanisms. Studies herein have demonstrated that androgens can regulate the PTGIR gene at a transcriptional level, which may in part account for some of the cardioprotection associated with androgens.

The more potent androgen DHT is synthesized from the metabolic conversion of testosterone by the enzyme 5 $\alpha$ -reductase. Conversely, testosterone is also a major biosource of estrogens, whereby testosterone can be aromatised to estradiol [71]. Therefore, it has been proposed that cardioprotection afforded by androgens could be mediated through aromatisation to estradiol and signalling through the ER [72]. Given that E<sub>2</sub> is a regulator of the PTGIR and the hIP promoter (PrmIP) contains a highly conserved functional ERE [23], the more active metabolite DHT which cannot be converted to estradiol by aromatase was used throughout this study. As a control, and to confirm that DHT cannot function through the ER, mutation of the functional ERE within PrmIP had no effect on PrmIP-directed gene expression following incubation with DHT, validating that the androgen response is independent of E<sub>2</sub>. These findings are in agreement with the role of the AR in atheroprotection [34], although AR-independent mechanisms cannot be ruled out.

As stated, androgens mainly exert their transcriptional effects by signalling through AR binding to target AREs [32]. The consensus sequence for most AREs, referred to as classical AREs (clAREs), is 5'-TGTTCT-3' arranged as inverted repeats separated by 3 nucleotide spacers [73]. Due to the similarity in the consensus sequences of clAREs and other nuclear receptor elements, such as the glucocorticoid receptor elements (GREs), progestin receptor elements (PREs) and mineralocorticoid receptor elements (MREs), these response elements are often described as 'promiscuous' as they represent possible binding sites for all four nuclear receptors [74]. However, there are a number of selective AREs (selAREs) found as partial direct repeats as opposed to inverted repeats of the 5'-TGTTTCT-3' consensus sequence, that can only bind the AR [73, 74]. In addition to the classical and selective AREs, studies have also identified ARE half-sites as AR binding targets. [75]. ChIP-on-ChIP experiments established that 50% of AR binding sites did not adhere to the known classical or selective consensus binding sites. Furthermore, ARE half-sites were found to be highly enriched in AR target promoters. Herein, bioinformatic analysis located a perfect consensus ARE half-site (5'-TGTTCT-3') within PrmIP and which is evolutionary conserved in other species, including in bovine, canine and rodent species. Genetic reporter assays confirmed that this novel half-site acts as a functional ARE, whereby mutation of this ARE completely abolished the DHT response on PrmIP-directed gene expression and ChIP analysis confirmed actual binding of the AR to PrmIP *in vivo*.

Additionally, androgens have previously been shown to upregulate expression of genes in conditions of reduced serum cholesterol through an SREBP/SRE-mediated mechanism [35]. In this established mechanism, stimulation with DHT leads to AR-dependent upregulation of the cholesterol-sensor SREBP cleavage activating protein (SCAP) which, in turn, leads to proteolytic cleavage of SREBP1 by site-1 protease (S1P) and S2P in the Golgi to liberate the mature, transcriptionally active basic helix-loop-helix leucine zipper (bHLH-LZ) domain of SREBP1 [37]. The mature SREBP1 is then free to translocate to the nucleus and bind to target SREs to direct transcriptional activation [76]. Hence, in situations of low cholesterol, DHT can regulate target gene expression via the direct AR-dependent mechanism and more indirectly, involving AR-dependent upregulation of SCAP1 and increased processing and activation of SREBP1. Notably, in the current study, it was demonstrated that DHT can upregulate PTGIR expression through the functional SRE within PrmIP in low cholesterol conditions, whereby disruption of this element resulted in marked decreases in PrmIP-directed gene expression. DHT stimulation also significantly increased SCAP mRNA expression. Immunofluorescence microscopy validated enhanced hIP expression in LCS/DHT-treated cells, while silencing of SREBP1 abolished this enhanced effect. This was corroborated by ChIP analysis where increased binding of SREBP1 to PrmIP was observed.

Hence, herein, we have established that DHT can regulate hIP expression and function in the vasculature through an AR-dependent transcriptional mechanism under normal cholesterol conditions. As indicated in the model in Figure 10a, it is proposed that in response to DHT-induced activation, the AR binds to the novel ARE within the core PrmIP upregulating PTGIR/hIP expression, and independent of the E<sub>2</sub>-ER $\alpha$ /ERE and the SREBP/SRE pathways. However, as depicted in Figure 10b, under low serum cholesterol conditions, it is proposed that DHT induction also leads to SREBP-mediated increases in gene expression, whereby stimulation with DHT increases SCAP expression and subsequent SREBP1 binding to PrmIP. Collectively, these data establish a role for low cholesterol and SREBP1 in the androgen-regulation of the PTGIR, confirming that DHT can work through both a direct AR-mediated mechanism and through an indirect mechanism involving enhanced SREBP1 binding to the PrmIP. Evidence in support of this model is given by the fact that mutation of the functional SRE reduced DHT-induced upregulation of PrmIP-directed luciferase expression in low serum cholesterol. Moreover, siRNA-mediated disruption of SREBP1 results in a significant loss ( $P < 0.0001$ ) of the DHT-mediated increase in hIP expression in low cholesterol conditions compared to the effects of siRNA<sub>CONTROL</sub> on hIP expression in cells treated with DHT cultured in low cholesterol serum. Furthermore, ChIP analyses indicated increased SREBP1 binding to PrmIP in cells cultured in low cholesterol serum and treated with DHT relative to binding observed in vehicle-treated cells cultured under the same conditions ( $P < 0.05$ ). It was notable that while conventional/end-point PCRs successfully generated PCR amplicons providing evidence of both AR and/or SREBP1 binding to the PrmIP, real-time PCR-based approaches for quantitation of such amplicons was not successful despite numerous attempts including involving a series of alternative primers and amplification conditions. Failure to generate such amplicons using real-time PCR approaches is most likely due to the fact that the region surrounding the ARE and SRE within PrmIP is predicted to have extensive hairpin structures, potentially interfering with certain PCR amplifications.

Previous studies have characterized the core promoter of the hIP gene/PTGIR [42], an upstream regulatory region [41], in addition to the functional ERE [23] and SRE [16]. We have demonstrated that similar to E<sub>2</sub> and low cholesterol, androgens can regulate the PTGIR through a transcriptional mechanism mediated by the AR/ARE in cells of a megakaryoblastic and endothelial lineage. In low-cholesterol conditions, DHT can also function through an SREBP1/SRE mechanism to further upregulate hIP expression. The study outlined herein not only provides a deeper understanding of the factors determining the transcriptional regulation of the PTGIR, but also reveal new insights into the possible protective effects of the prostacyclin/IP axis. In view of such protective roles of prostacyclin and the IP in the vasculature, it is indeed possible that this upregulation of IP expression might, at least in part, explain the widely reported cardioprotective effects of androgens. Given that the nature of androgenic protection within the vasculature may occur through numerous 'direct' and 'indirect' pathways [46, 47, 48, 49], this study provides one

Regulated Expression of the Prostacyclin Receptor (IP) Gene by Androgens within the Vasculature: Combined role for Androgens and Serum Cholesterol. Eivers SB & **Kinsella BT**. (2016) *Biochim Biophys Acta (Gene Regulatory Mechanisms)*, **1859(10)**, p1333-1351.

possible AR-dependent mechanism for cardioprotection. Although the use of androgens as a possible therapeutic in cardiovascular disease is contentious, more detailed scrutiny of the clinical relationship between androgens and the COX/prostacyclin pathway in the vasculature is warranted, including in clinical settings involving androgen-deprivation therapy. Furthermore, the fact that the hIP is up-regulated by androgens and low cholesterol in both platelet progenitor megakaryoblastic and vascular endothelial lineages suggests that these factors/conditions may confer both *anti*-thrombotic benefits in addition to endothelial benefits in reducing the risk of coronary artery disease in men.

#### References

1. Bunting, S., et al., *Arterial walls generate from prostaglandin endoperoxides a substance (prostaglandin X) which relaxes strips of mesenteric and coeliac arteries and inhibits platelet aggregation*. *Prostaglandins*, 1976. **12**(6): p. 897-913.
2. Hayes, J.S., et al., *The prostacyclin receptor is isoprenylated. Isoprenylation is required for efficient receptor-effector coupling*. *J Biol Chem*, 1999. **274**(34): p. 23707-18.
3. Reid, H.M., et al., *Interaction of the human prostacyclin receptor with Rab11: characterization of a novel Rab11 binding domain within alpha-helix 8 that is regulated by palmitoylation*. *J Biol Chem*, 2010. **285**(24): p. 18709-26.
4. Cheng, Y., et al., *Role of prostacyclin in the cardiovascular response to thromboxane A2*. *Science*, 2002. **296**(5567): p. 539-41.
5. Fitzgerald, G.A., *Coxibs and cardiovascular disease*. *N Engl J Med*, 2004. **351**(17): p. 1709-11.
6. Christman, B.W., et al., *An imbalance between the excretion of thromboxane and prostacyclin metabolites in pulmonary hypertension*. *N Engl J Med*, 1992. **327**(2): p. 70-5.
7. Stitham, J., et al., *Prostacyclin: an inflammatory paradox*. *Front Pharmacol*, 2011. **2**: p. 24.
8. Stitham, J., et al., *Comprehensive biochemical analysis of rare prostacyclin receptor variants: study of association of signaling with coronary artery obstruction*. *J Biol Chem*, 2011. **286**(9): p. 7060-9.
9. Arehart, E., et al., *Acceleration of cardiovascular disease by a dysfunctional prostacyclin receptor mutation: potential implications for cyclooxygenase-2 inhibition*. *Circ Res*, 2008. **102**(8): p. 986-93.
10. Murata, T., et al., *Altered pain perception and inflammatory response in mice lacking prostacyclin receptor*. *Nature*, 1997. **388**(6643): p. 678-82.
11. Hoshikawa, Y., et al., *Prostacyclin receptor-dependent modulation of pulmonary vascular remodeling*. *Am J Respir Crit Care Med*, 2001. **164**(2): p. 314-8.
12. Kawabe, J., et al., *Prostaglandin I2 promotes recruitment of endothelial progenitor cells and limits vascular remodeling*. *Arterioscler Thromb Vasc Biol*, 2010. **30**(3): p. 464-70.
13. Reid, H.M. and B.T. Kinsella, *Prostacyclin receptors: Transcriptional regulation and novel signalling mechanisms*. *Prostaglandins Other Lipid Mediat*, 2015. **121**(Pt A): p. 70-82.
14. Vogel, R.A., *Cholesterol lowering and endothelial function*. *Am J Med*, 1999. **107**(5): p. 479-87.
15. Smith, L.H., et al., *Cyclooxygenase-2-dependent prostacyclin formation is regulated by low density lipoprotein cholesterol in vitro*. *Arterioscler Thromb Vasc Biol*, 2002. **22**(6): p. 983-8.
16. Turner, E.C. and B.T. Kinsella, *Regulation of the human prostacyclin receptor gene by the cholesterol-responsive SREBP1*. *J Lipid Res*, 2012. **53**(11): p. 2390-404.
17. Tostes, R.C., et al., *Effects of estrogen on the vascular system*. *Braz J Med Biol Res*, 2003. **36**(9): p. 1143-58.
18. Collins, P., et al., *17 beta-Estradiol attenuates acetylcholine-induced coronary arterial constriction in women but not men with coronary heart disease*. *Circulation*, 1995. **92**(1): p. 24-30.
19. Bourassa, P.A., et al., *Estrogen reduces atherosclerotic lesion development in apolipoprotein E-deficient mice*. *Proc Natl Acad Sci U S A*, 1996. **93**(19): p. 10022-7.
20. Orshal, J.M. and R.A. Khalil, *Gender, sex hormones, and vascular tone*. *Am J Physiol Regul Integr Comp Physiol*, 2004. **286**(2): p. R233-49.
21. Ospina, J.A., D.N. Krause, and S.P. Duckles, *17beta-estradiol increases rat cerebrovascular prostacyclin synthesis by elevating cyclooxygenase-1 and prostacyclin synthase*. *Stroke*, 2002. **33**(2): p. 600-5.
22. Egan, K.M., et al., *COX-2-derived prostacyclin confers atheroprotection on female mice*. *Science*, 2004. **306**(5703): p. 1954-7.
23. Turner, E.C. and B.T. Kinsella, *Estrogen increases expression of the human prostacyclin receptor within the vasculature through an ERalpha-dependent mechanism*. *J Mol Biol*, 2010. **396**(3): p. 473-86.
24. Herring, M.J., et al., *Testosterone and the cardiovascular system: a comprehensive review of the basic science literature*. *J Am Heart Assoc*, 2013. **2**(4): p. e000271.
25. Traish, A.M., et al., *The dark side of testosterone deficiency: III. Cardiovascular disease*. *J Androl*, 2009. **30**(5): p. 477-94.
26. Kelly, D.M. and T.H. Jones, *Testosterone: a vascular hormone in health and disease*. *J Endocrinol*, 2013. **217**(3): p. R47-71.
27. Jones, T.H., *Testosterone deficiency: a risk factor for cardiovascular disease?* *Trends Endocrinol Metab*, 2010. **21**(8): p. 496-503.
28. Shahani, S., M. Braga-Basaria, and S. Basaria, *Androgen deprivation therapy in prostate cancer and metabolic risk for atherosclerosis*. *J Clin Endocrinol Metab*, 2008. **93**(6): p. 2042-9.
29. Crawford, E.D. and J.W. Moul, *ADT risks and side effects in advanced prostate cancer: cardiovascular and acute renal injury*. *Oncology (Williston Park)*, 2015. **29**(1): p. 55-8, 65-6.
30. Laughlin, G.A., E. Barrett-Connor, and J. Bergstrom, *Low serum testosterone and mortality in older men*. *J Clin Endocrinol Metab*, 2008. **93**(1): p. 68-75.

31. Ohlsson, C., et al., *High serum testosterone is associated with reduced risk of cardiovascular events in elderly men. The MrOS (Osteoporotic Fractures in Men) study in Sweden.* J Am Coll Cardiol, 2011. **58**(16): p. 1674-81.
32. Li, J. and F. Al-Azzawi, *Mechanism of androgen receptor action.* Maturitas, 2009. **63**(2): p. 142-8.
33. Lee, H.J. and C. Chang, *Recent advances in androgen receptor action.* Cell Mol Life Sci, 2003. **60**(8): p. 1613-22.
34. Bourghardt, J., et al., *Androgen receptor-dependent and independent atheroprotection by testosterone in male mice.* Endocrinology, 2010. **151**(11): p. 5428-37.
35. Heemers, H.V., G. Verhoeven, and J.V. Swinnen, *Androgen activation of the sterol regulatory element-binding protein pathway: Current insights.* Mol Endocrinol, 2006. **20**(10): p. 2265-77.
36. Heemers, H., et al., *Androgens stimulate lipogenic gene expression in prostate cancer cells by activation of the sterol regulatory element-binding protein cleavage activating protein/sterol regulatory element-binding protein pathway.* Mol Endocrinol, 2001. **15**(10): p. 1817-28.
37. Heemers, H., et al., *Identification of an androgen response element in intron 8 of the sterol regulatory element-binding protein cleavage-activating protein gene allowing direct regulation by the androgen receptor.* J Biol Chem, 2004. **279**(29): p. 30880-7.
38. Wen, J., H. Zhu, and P.C. Leung, *Gonadal steroids regulate the expression of aggrecanases in human endometrial stromal cells in vitro.* J Cell Mol Med, 2013. **17**(10): p. 1325-34.
39. Boutin, B., et al., *Androgen deprivation and androgen receptor competition by bicalutamide induce autophagy of hormone-resistant prostate cancer cells and confer resistance to apoptosis.* Prostate, 2013. **73**(10): p. 1090-102.
40. Cochrane, D.R., et al., *Role of the androgen receptor in breast cancer and preclinical analysis of enzalutamide.* Breast Cancer Res, 2014. **16**(1): p. R7.
41. Keating, G.L., E.C. Turner, and B.T. Kinsella, *Regulation of the human prostacyclin receptor gene in megakaryocytes: Major roles for C/EBPdelta and PU.1.* Biochim Biophys Acta, 2012. **1819**(5): p. 428-445.
42. Turner, E.C. and B.T. Kinsella, *Transcriptional regulation of the human prostacyclin receptor gene is dependent on Sp1, PU.1 and Oct-1 in megakaryocytes and endothelial cells.* J Mol Biol, 2009. **386**(3): p. 579-97.
43. Metzger, E., et al., *Phosphorylation of histone H3 at threonine 11 establishes a novel chromatin mark for transcriptional regulation.* Nat Cell Biol, 2008. **10**(1): p. 53-60.
44. Yuhki, K., et al., *Roles of prostanoids in the pathogenesis of cardiovascular diseases: Novel insights from knockout mouse studies.* Pharmacol Ther, 2011. **129**(2): p. 195-205.
45. Turner, E.C., et al., *Interaction of the human prostacyclin receptor with the PDZ adapter protein PDZK1: role in endothelial cell migration and angiogenesis.* Mol Biol Cell, 2011. **22**(15): p. 2664-79.
46. Quandt, K., et al., *MatInd and MatInspector: new fast and versatile tools for detection of consensus matches in nucleotide sequence data.* Nucleic Acids Res, 1995. **23**(23): p. 4878-84.
47. Nichols, M., et al., *Cardiovascular disease in Europe 2014: epidemiological update.* Eur Heart J, 2014. **35**(42): p. 2929.
48. Lozano, R., et al., *Global and regional mortality from 235 causes of death for 20 age groups in 1990 and 2010: a systematic analysis for the Global Burden of Disease Study 2010.* Lancet, 2012. **380**(9859): p. 2095-128.
49. Basaria, S., et al., *Adverse events associated with testosterone administration.* N Engl J Med, 2010. **363**(2): p. 109-22.
50. Sullivan, M.L., et al., *The cardiac toxicity of anabolic steroids.* Prog Cardiovasc Dis, 1998. **41**(1): p. 1-15.
51. Hatakeyama, H., et al., *Testosterone inhibits tumor necrosis factor-alpha-induced vascular cell adhesion molecule-1 expression in human aortic endothelial cells.* FEBS Lett, 2002. **530**(1-3): p. 129-32.
52. Svartberg, J., et al., *Association of endogenous testosterone with blood pressure and left ventricular mass in men. The Tromso Study.* Eur J Endocrinol, 2004. **150**(1): p. 65-71.
53. Somjen, D., et al., *Effects of gonadal steroids and their antagonists on DNA synthesis in human vascular cells.* Hypertension, 1998. **32**(1): p. 39-45.
54. Bruck, B., et al., *Gender-specific differences in the effects of testosterone and estrogen on the development of atherosclerosis in rabbits.* Arterioscler Thromb Vasc Biol, 1997. **17**(10): p. 2192-9.
55. Funk, C.D. and G.A. FitzGerald, *COX-2 inhibitors and cardiovascular risk.* J Cardiovasc Pharmacol, 2007. **50**(5): p. 470-9.
56. Kirkby, N.S., et al., *Cyclooxygenase-1, not cyclooxygenase-2, is responsible for physiological production of prostacyclin in the cardiovascular system.* Proc Natl Acad Sci U S A, 2012. **109**(43): p. 17597-602.
57. Guo, Y., et al., *The COX-2/PGI2 receptor axis plays an obligatory role in mediating the cardioprotection conferred by the late phase of ischemic preconditioning.* PLoS One, 2012. **7**(7): p. e41178.
58. Narumiya, S. and T. Furuyashiki, *Fever, inflammation, pain and beyond: prostanoid receptor research during these 25 years.* FASEB J, 2011. **25**(3): p. 813-8.
59. Cheuk, B.L., et al., *Androgen control of cyclooxygenase expression in the rat epididymis.* Biol Reprod, 2000. **63**(3): p. 775-80.

60. Yazawa, T., et al., *Androgen/androgen receptor pathway regulates expression of the genes for cyclooxygenase-2 and amphiregulin in periovulatory granulosa cells*. *Mol Cell Endocrinol*, 2013. **369**(1-2): p. 42-51.
61. Osterlund, K.L., R.J. Handa, and R.J. Gonzales, *Dihydrotestosterone alters cyclooxygenase-2 levels in human coronary artery smooth muscle cells*. *Am J Physiol Endocrinol Metab*, 2010. **298**(4): p. E838-45.
62. Marrachelli, V.G., et al., *Role of NO-synthases and cyclooxygenases in the hyperreactivity of male rabbit carotid artery to testosterone under experimental diabetes*. *Pharmacol Res*, 2010. **61**(1): p. 62-70.
63. Chng, K.R., et al., *A transcriptional repressor co-regulatory network governing androgen response in prostate cancers*. *EMBO J*, 2012. **31**(12): p. 2810-23.
64. Yue, P., et al., *Testosterone relaxes rabbit coronary arteries and aorta*. *Circulation*, 1995. **91**(4): p. 1154-60.
65. Heinlein, C.A. and C. Chang, *The roles of androgen receptors and androgen-binding proteins in nongenomic androgen actions*. *Mol Endocrinol*, 2002. **16**(10): p. 2181-7.
66. Jones, R.D., et al., *The vasodilatory action of testosterone: a potassium-channel opening or a calcium antagonistic action?* *Br J Pharmacol*, 2003. **138**(5): p. 733-44.
67. Perusquia, M., et al., *Regional differences in the vasorelaxing effects of testosterone and its 5-reduced metabolites in the canine vasculature*. *Vascul Pharmacol*, 2012. **56**(3-4): p. 176-82.
68. Campelo, A.E., P.H. Cutini, and V.L. Massheimer, *Cellular actions of testosterone in vascular cells: mechanism independent of aromatization to estradiol*. *Steroids*, 2012. **77**(11): p. 1033-40.
69. Bishop-Bailey, D., *The platelet as a model system for the acute actions of nuclear receptors*. *Steroids*, 2010. **75**(8-9): p. 570-5.
70. Goglia, L., et al., *Endothelial regulation of eNOS, PAI-1 and t-PA by testosterone and dihydrotestosterone in vitro and in vivo*. *Mol Hum Reprod*, 2010. **16**(10): p. 761-9.
71. Liu, P.Y., A.K. Death, and D.J. Handelsman, *Androgens and cardiovascular disease*. *Endocr Rev*, 2003. **24**(3): p. 313-40.
72. Nathan, L., et al., *Testosterone inhibits early atherogenesis by conversion to estradiol: critical role of aromatase*. *Proc Natl Acad Sci U S A*, 2001. **98**(6): p. 3589-93.
73. Claessens, F., et al., *Selective DNA binding by the androgen receptor as a mechanism for hormone-specific gene regulation*. *J Steroid Biochem Mol Biol*, 2001. **76**(1-5): p. 23-30.
74. Claessens, F., et al., *Diverse roles of androgen receptor (AR) domains in AR-mediated signaling*. *Nucl Recept Signal*, 2008. **6**: p. e008.
75. Massie, C.E., et al., *New androgen receptor genomic targets show an interaction with the ETS1 transcription factor*. *EMBO Rep*, 2007. **8**(9): p. 871-8.
76. Horton, J.D., J.L. Goldstein, and M.S. Brown, *SREBPs: activators of the complete program of cholesterol and fatty acid synthesis in the liver*. *J Clin Invest*, 2002. **109**(9): p. 1125-31.

**Figure Legends:**

**Figure 1: Effect of DHT on hIP mRNA and PrmIP-directed gene expression**

**Panels A-D:** Quantitative reverse transcriptase (qRT)-PCR analysis of hIP mRNA expression in HEL 92.1.7 (**Panels A & C**) and EA.hy926 (**Panels B & D**) cells incubated for 24 hr with 10 nM 5 $\alpha$ -dihydrotestosterone (DHT), 100 nM hydroxyflutamide (HF), 10 nM Estrogen (E<sub>2</sub>), 100 nM ICI 182,780 (ICI), 100 nM cycloheximide (CHX), 10  $\mu$ g/ml actinomycin D (Act D), either alone or in combination, or with the drug vehicle (V; 0.01% EtOH). Data is presented as mean hIP mRNA expression ( $\pm$  SEM, n =3) relative to levels in vehicle-treated cells, set to a value of 1. The asterisks indicate that DHT significantly increased hIP mRNA expression. The hashes indicate that the antagonists/inhibitors reduced the DHT induction, where\*/#, \*\*/##, \*\*\* and \*\*\*\* signify  $P \leq 0.05$ , 0.01, 0.001 and 0.0001, respectively. **Panels E -G:** HEL cells were co-transfected with pRL-TK along with pGL3B:PrmIP (**Panel E**) or pGL3B:PrmIP6 (**Panels F & G**). Some 24 hr post-transfection, cells were incubated for 24 hr with 0 - 50 nM DHT alone or 10 nM DHT plus 100 nM HF, 50  $\mu$ M bicalutamide (BIC) or 10  $\mu$ M enzalutamide (ENZ) or with the drug vehicle (V; 0.01% EtOH) prior to measurement of firefly and renilla luciferase activity. Data is presented as mean firefly relative to renilla luciferase activity (RLU  $\pm$  SEM, n =3). The asterisks show that DHT significantly increased the levels of firefly luciferase reporter gene expression or that the antagonists reduced the DHT induction, where \*, \*\*, \*\*\* and \*\*\*\* signify  $P \leq 0.05$ , 0.01, 0.001 and 0.0001, respectively.

**Figure 2: Effect of DHT on agonist-induced cAMP generation by the hIP.**

**Panels A-D:** HEL (**Panels A & B**) and EA.hy926 (**Panels C & D**) cells were transiently co-transfected with pCRE-Luc plus pRL-TK. Some 48 hr post-transfection, cells were incubated for 24 hr either with 10 nM DHT, 10 nM E<sub>2</sub>, 10 nM DHT plus 100 nM HF, 10 nM E<sub>2</sub> plus 100 nM ICI, or with the vehicle (0.01% EtOH). Thereafter, cells were pre-incubated with 100  $\mu$ M IBMX for 30 min and then stimulated for 3 hr with either 1  $\mu$ M Cicaprost or vehicle (0.01% EtOH) prior to measurement of firefly and renilla luciferase activities. Data in (**A & C**) are presented as cAMP accumulation in vehicle or Cicaprost-stimulated cells (RLU  $\pm$  SEM, n = 3) or in (**B & D**) as fold increase in cAMP accumulation. The asterisks indicate that DHT significantly increased the levels of Cicaprost-induced cAMP generation where \*\*\*\* signifies  $P \leq 0.0001$ .

**Panels E & F:** Migration after scratch wounds in EA.hy926 cell monolayers preincubated for 24 hr with DHT (10 nM) or vehicle (0.01% EtOH), prior to stimulation with Cicaprost (1  $\mu$ M) or drug vehicle (0.01% EtOH) in the presence or absence of RO1138452 (RO; 10  $\mu$ M). Bar charts (**Panel F**) represent mean percentage wound closure ( $\pm$  SEM, n=4). The asterisks (\*) indicate Cicaprost increased EA.hy926 cell migration while the \$ symbols signifies that the IP antagonist RO1138452 significantly reduced Cicaprost-induced EC migration (one-way ANOVA analyses in both cases, where \*\*\*\*/\$\$\$\$ signifies  $P \leq 0.0001$ , respectively). The # symbol indicates that the levels of Cicaprost-induced cell migration in cells preincubated for 24 hr with DHT was significantly increased relative to that in cells preincubated with the drug vehicle for one-way ANOVA analysis followed by post-hoc Bonferroni multiple comparison *t*-test analysis, where # signifies  $P < 0.05$ .

**Figure 3: Effect of DHT on hIP expression in 1°HUVECs.**

**Panels A & B:** qRT-PCR analysis of hIP mRNA expression in 1°HUVECs incubated for 24 hr with 10 nM DHT, 100 nM HF, 10 nM E<sub>2</sub>, 100 nM ICI, 100 nM CHX, 10  $\mu$ g/ml Act D, either alone or in combination, or with the drug vehicle (V; 0.01% EtOH). Data is presented as mean hIP mRNA expression ( $\pm$  SEM, n =3) relative to levels in vehicle-treated cells, set to a value of 1. The asterisks indicate that DHT significantly increased hIP mRNA expression. The hashes indicate that the antagonists/inhibitors reduced the DHT induction, where #/\*, \*\*, ### and \*\*\*\* signify  $P \leq 0.05$ , 0.01, 0.001 and 0.0001, respectively. **Panel C:** 1°HUVECs were incubated for 24 hr with drug vehicle (0.01% EtOH), 10 nM DHT, or DHT in the presence of 100 nM HF, 50  $\mu$ M BIC, 10  $\mu$ M ENZ where cells incubated with 10 nM E<sub>2</sub> served as a reference positive control. For immunofluorescence microscopy, cells were then immunolabelled with the 1° anti-hIP serum and 2° Alexa-Fluor 488-conjugated anti-rabbit IgG (green), followed by counterstaining with DAPI (blue).

To validate specificity, the *anti*-hIP serum was pre-incubated with the antigenic IC<sub>2</sub> peptide (10 µg/ml) prior to immunolabelling of cells while as an additional negative control, cells were labelled with the Alexa Fluor 488-conjugated *anti*-rabbit IgG in the absence of the 1° *anti*-hIP serum. Images were captured at 63x with a Zeiss microscope and Axioplan software. **Panel D:** Bar chart shows levels of hIP expression, expressed as the corrected total cell fluorescence (CTCF;  $\times 10^6$ ), where quantification was carried out using ImageJ and the formula:  $CTCF = \text{Integrated density} - (\text{Area of cell} \times \text{Mean background fluorescence})$ . The asterisks indicate where DHT or E<sub>2</sub> significantly increased hIP expression relative to vehicle treatment. The hashes indicate where co-incubation with the AR antagonists HF, BIC or ENZ significantly decreased DHT induction in hIP expression, where \*/#, \*\*/### and ###/### signify  $P \leq 0.05, 0.01$  and  $0.001$ , respectively, for one-way ANOVA analysis followed by post-hoc Bonferroni multiple comparison *t*-test analysis.

**Figure 4: Localization of the androgen-responsive region (ARR) within PrmIP by 5' deletional analysis.**

A schematic of the human PTGIR genomic region, spanning nucleotides -2449 to +767 and encoding PrmIP, exon (E)1, intron (I) 1 and E2, is shown above each panel where +1 corresponds to the translational initiation site. HEL (**Panel A**), EA.hy 926 (**Panel B**) cells and 1°HUVECs (**Panel C**) were co-transfected with pRL-TK along with pGL3B plasmids encoding PrmIP, PrmIP1-PrmIP7 or, as positive controls, encoding the PSA or MMTV promoters. Some 24 hr post-transfection, cells were incubated for 24 hr with vehicle (0.01% EtOH) or 10 nM DHT prior to measurement of firefly and renilla luciferase activity. Data is presented as mean firefly relative to renilla luciferase activity ( $RLU \pm SEM, n = 3$ ). The asterisks show that DHT significantly increased the levels of firefly luciferase reporter gene expression where \*\*, \*\*\* and \*\*\*\* signify  $P \leq 0.01, 0.001$  and  $0.0001$ , respectively. Through 5' deletional analysis, the androgen-responsive region (ARR) was localized to nucleotides -1042 to -917 (between PrmIP6 and PrmIP7), as indicated.

**Figure 5: Identification of a putative ARE within PrmIP.**

A schematic of PrmIP2 (**Panels A – C**) and PrmIP6 (**Panels D – F**) indicating the location of the functional ERE, SRE and putative ARE, where the 5' nucleotide of each element is indicated and the star symbol indicates mutated elements. HEL (**Panels A & D**), EA.hy 926 (**Panels B & E**) cells and 1°HUVECs (**Panels C & F**) were co-transfected with pRL-TK along with pGL3B encoding either PrmIP2, PrmIP6, or their mutated ERE\*, SRE\* and ARE\* variants. Some 24 hr post-transfection, cells were incubated for 24 hr with vehicle (0.01% EtOH) or 10 nM DHT prior to measurement of firefly and renilla luciferase activity. Data is presented as mean firefly relative to renilla luciferase activity ( $RLU \pm SEM, n = 3$ ). The asterisks show that DHT significantly increased the levels of firefly luciferase reporter gene expression, and the hashes show that this increase is reduced by mutating the putative ARE, where \*\*\* and \*\*\*\*/##### signify  $P \leq 0.001$  and  $0.0001$ , respectively.

**Figure 6: Effects of CHO and DHT on PrmIP-directed gene expression.**

A schematic of PrmIP2 and PrmIP6 indicating the location of the functional SRE and putative ARE is given above each panel, where the 5' nucleotide of each element is indicated and the star symbol indicates mutated elements. HEL (**Panels A-C**) and EA.hy 926 (**Panels D-F**) cells were cultured for 24 hr in either normal serum (NS) or low cholesterol serum (LCS) and co-transfected with pRL-TK along with pGL3B encoding either PrmIP2, PrmIP6, or their mutated SRE\* and ARE\* variants. In **Panels A & D**, cells were harvested 48 hr post-transfection while in **Panels B, C, E & F** at 24 hr post-transfection, cells were incubated for an additional 24 hr with vehicle (0.01% EtOH) or 10 nM DHT prior to measurement of firefly and renilla luciferase activity. All data is presented as mean firefly relative to renilla luciferase activity ( $RLU \pm SEM, n = 3$ ). The asterisks indicate where LCS or DHT significantly increased while the hashes indicate where mutating the putative ARE or SRE significant decreased levels of firefly luciferase reporter gene expression, where \*\*\* and \*\*\*\*/##### signify  $P \leq 0.001$  and  $0.0001$ , respectively.

**Figure 7: Effect of DHT in SCAP mRNA expression**

**Panel A & B:** qRT-PCR analysis of SCAP mRNA expression in HEL (**Panel A**) and EA.hy926 (**Panel B**) cells cultured for 24 hr in either normal serum (NS) or low cholesterol serum (LCS), prior to incubation for 24 hr with 10 nM DHT, 10 nM DHT plus 100 nM HF, 10 nM DHT plus 50  $\mu$ M BIC, 10 nM DHT plus 10  $\mu$ M ENZ or with the drug vehicle (V; 0.01% EtOH). Data is presented as mean SCAP mRNA expression ( $\pm$  SEM, n =3) relative to levels in vehicle-treated cells, set to a value of 1. The asterisks indicate that DHT significantly increased SCAP mRNA expression, where \*, \*\*\*\* signifies  $P \leq 0.05$  and 0.0001, respectively.

**Figure 8: Effect of siRNA-disruption of AR and SREBP1 on hIP expression**

**Panel A & B:** 1<sup>o</sup> HUVECs, cultured for 24 hr in either normal serum (NS; **Panel A**) or low cholesterol serum (LCS; **Panel B**), were transfected with siRNAs directed to the AR (siRNA<sub>AR</sub>), SREBP (siRNA<sub>SREBP1</sub>) or to a scrambled control sequence (siRNA<sub>CONTROL</sub>), where non-transfected cells acted as a reference control. Some 72 hr post-transfection, cells were incubated for 24 hr with 10 nM DHT or vehicle (v; 0.01% EtOH) prior to analysis by immunofluorescence microscopy. Cells were fixed and immunolabelled with anti-hIP sera and Alexa-Fluor 488-conjugated anti-rabbit IgG (green), followed by counterstaining with DAPI (blue). Images were captured at 63x with a Zeiss microscope and Axioplan software. **Panel C:** Bar chart shows levels of hIP expression, expressed as the corrected total cell fluorescence (CTCF;  $\times 10^6$ ), where quantification was carried out using ImageJ and the formula: CTCF = Integrated density – (Area of cell  $\times$  Mean background fluorescence). The asterisks indicate where DHT significantly increased hIP expression relative to vehicle treatment or where cholesterol depletion resulted in significant increases in hIP expression relative to those in normal cholesterol levels. The hashes indicate where siRNA mediated disruption of the AR or SREBP1 significantly decreased DHT induction in hIP expression. \*\* & #####/\*\*\*\* signifies  $P \leq 0.01$  &  $P \leq 0.0001$  respectively, for one-way ANOVA analysis followed by post-hoc Bonferroni multiple comparison *t*-test analysis. **Panel D:** Immunoblot analysis of AR and SREBP1 expression in whole cell lysates (20  $\mu$ g/lane) of 1<sup>o</sup> HUVECs cultured for 24 hr in normal serum and transfected for 96 hr either with the respective target/control siRNA, where non-transfected cells served as a reference. To verify uniform protein loading, immunoblots were screened with anti-HDJ2 antibody for assessment of the internal loading control HDJ2. Data presented is representative of at least 3 independent experiments. The relative positions of the molecular size markers (kDa) are on the left of the panels-

**Figure 9: ChIP analysis of AR binding to PrmIP.**

**Panel A & B:** A schematic of the PTGIR (nucleotides -2427 to -772) showing relative positions of the putative ARE (-978) and functional SRE (-937) within the PrmIP, where the solid arrows represent primers used to amplify the test androgen-responsive region (nucleotides -1019 to -841). As a negative control, the region spanning nucleotides -7718 to -7610 of the TBXA2R gene was amplified, where the dashed arrows represent primers used to amplify this control region. EA.hy926 cells were cultured for 24 hr in normal serum (NS) or low cholesterol serum (LCS), prior to incubation with 10 nM DHT or the drug vehicle (0.01% EtOH), crosslinking and chromatin extraction. For ChIP analysis of AR or SREBP1 binding, either input chromatin or chromatin extracted from anti-AR, anti-SREBP1, normal rabbit IgG or no 1<sup>o</sup> antibody control (-AB) immunoprecipitates was subjected to PCR analysis to amplify either the test (Panel A) or control (Panel B) regions. **Panel C:** Bar chart shows densitometric quantitation of PCR amplicons generated from the SREBP1 and AR immunoprecipitates ( $\pm$  SEM; n=3) relative to those derived from the corresponding input chromatins. The asterisks indicate where incubation with DHT resulted in significant increases in amplicons generated relative to those incubated with vehicle, where \* signifies  $P \leq 0.05$  for one-way ANOVA analysis followed by post-hoc Bonferroni multiple comparison *t*-test analysis.

**Figure 10: Mechanism of androgen regulation of hIP expression.**

**Panel A:** In normal serum conditions, DHT stimulation leads to release of heat shock proteins (HSPs) from a complex with the AR, promoting AR-phosphorylation, homodimerisation, nuclear translocation and transcriptional activation of androgen-responsive target genes. Hence, following activation, the AR binds to the novel ARE within the PrmIP of the PTGIR, directing increased hIP mRNA and protein expression. In conditions of normal serum cholesterol, SREBP1 binds at lower levels to the SRE as depicted by the broken circle around SREBP1 in the model. **Panel B:** In low cholesterol conditions, in addition to AR binding to the ARE, stimulation with DHT can also result in SREBP1 binding to the SRE within PrmIP, increasing hIP expression, which occurs through an established mechanism involving AR-dependent upregulated expression of the cholesterol-responsive SCAP. This increase in SCAP escorts SREBP1 from the ER to the Golgi apparatus to facilitate site-1 protease (S1P)- and S2P- processing and release of the basic helix-loop-helix domain of SREBP1. The mature, transcriptionally active SREBP1, in turn, translocates to the nucleus and can bind *cis*-acting SREs to increase target gene expression, such as of the PTGIR/IP.

**Supplemental Figures:**

**Supplemental Figure 1: Effect of DHT on hIP mRNA expression and PrmIP6-directed gene expression**

**Panels A & B:** qRT-PCR analysis of hIP mRNA expression in HEL 92.1.7 (**Panel A**) and EA.hy926 (**Panel B**) cells incubated for 24 hr with 0, 5, 10, 50, 100 or 200 nM DHT. Data is presented as mean hIP mRNA expression ( $\pm$  SEM,  $n=3$ ) relative to levels in vehicle-treated cells, set to a value of 1. The asterisks indicate that DHT significantly increased hIP mRNA expression. where \*\* and \*\*\*\* signify  $P \leq 0.01$  and  $0.0001$ , respectively. **Panel C:** EA.hy926 cells were co-transfected with pRL-TK along with pGL3B:PrmIP6. Some 24 hr post-transfection, cells were incubated for 24 hr with 0 - 50 nM DHT prior to measurement of firefly and renilla luciferase activity. Data is presented as mean firefly relative to renilla luciferase activity ( $RLU \pm$  SEM,  $n=3$ ). The asterisks show that DHT significantly increased the levels of firefly luciferase reporter gene expression or that the antagonists reduced the DHT induction, where \*, \*\*, \*\*\* and \*\*\*\* signify  $P \leq 0.05$ ,  $0.01$ ,  $0.001$  and  $0.0001$ , respectively.

**Supplemental Figure 2: Localisation of the androgen responsive region within PrmIP**

A schematic of the PTGIR genomic region spanning nucleotides -2449 to +767, encoding PrmIP, exon (E)1, intron (I) 1 and E2, where +1 corresponds to the translational initiation site. HEL cells (**Panel A**), EA.hy 926 cells (**Panel B**) and 1<sup>o</sup> HUVECs (**Panel C**) were co-transfected with pRL-TK along with pGL3B encoding either PrmIP or its 5' deletion derivatives PrmIP1-PrmIP7 or, as positive controls, pGL3:PSA or pGL3:MMTV. Some 24 hr post-transfection, cells were incubated for 24 hr with either vehicle (0.01% EtOH) or 10 nM DHT prior to measurement of firefly and renilla luciferase activity. Data is presented as mean fold induction of luciferase expression in DHT- relative to vehicle-treated cells ( $RLU \pm$  SEM,  $n=3$ ). The asterisks show that DHT significantly increased the levels of firefly luciferase reporter gene expression where \*\*\* and \*\*\*\* signify  $P \leq 0.001$  and  $0.0001$ , respectively.

**Supplemental Figure 3: Effects of E<sub>2</sub> on the putative ARE within PrmIP**

A schematic of PrmIP2 (**Panels A & B**) indicating the location of the functional ERE and putative ARE, where the 5' nucleotide of each element is indicated and the star symbol indicates mutated elements. HEL (**Panel A**) and EA.hy 926 (**Panel B**) cells were co-transfected with pRL-TK along with pGL3B encoding either PrmIP2, PrmIP6, or their mutated ERE\* and ARE\* variants. Some 24 hr post-transfection, cells were incubated for 24 hr with vehicle (0.01% EtOH) or 10 nM E<sub>2</sub> prior to measurement of firefly and renilla luciferase activity. Data is presented as mean firefly relative to renilla luciferase activity ( $RLU \pm$  SEM,  $n=3$ ). The asterisks show that E<sub>2</sub> significantly increased the levels of firefly luciferase reporter gene expression where \*\*\*\* signifies  $P \leq 0.0001$ . Note, mutating the ERE and not the ARE, blocked the E<sub>2</sub>-increase in PrmIP2-induced luciferase expression.

**Supplemental Figure 4: ChIP analysis of AR binding to PrmIP.**

EA.hy926 cells were cultured for 24 hr in normal serum (NS) or low cholesterol serum (LCS) prior to incubation with 10 nM DHT or the drug vehicle (0.01% EtOH), crosslinking and chromatin extraction. For ChIP analysis of AR or SREBP1 binding, either input chromatin or chromatin extracted from *anti-AR*, *anti-SREBP1*, normal rabbit IgG or no 1<sup>o</sup> antibody control (-AB) immunoprecipitates was subjected to PCR analysis to amplify either the test (**Panels A & B**) or control (**Panels C & D**) regions. Bar charts show densitometric quantitation of PCR amplicons generated from the individual SREBP1 and AR immunoprecipitates ( $\pm$  SEM; n=3) relative to those derived from the corresponding input chromatins. The asterisks indicate where incubation with DHT resulted in significant increases in amplicons generated relative to those incubated with vehicle, where \* signifies  $P \leq 0.05$  for one-way ANOVA analysis followed by post-hoc Bonferroni multiple comparison *t*-test analysis.

**Figure 1**

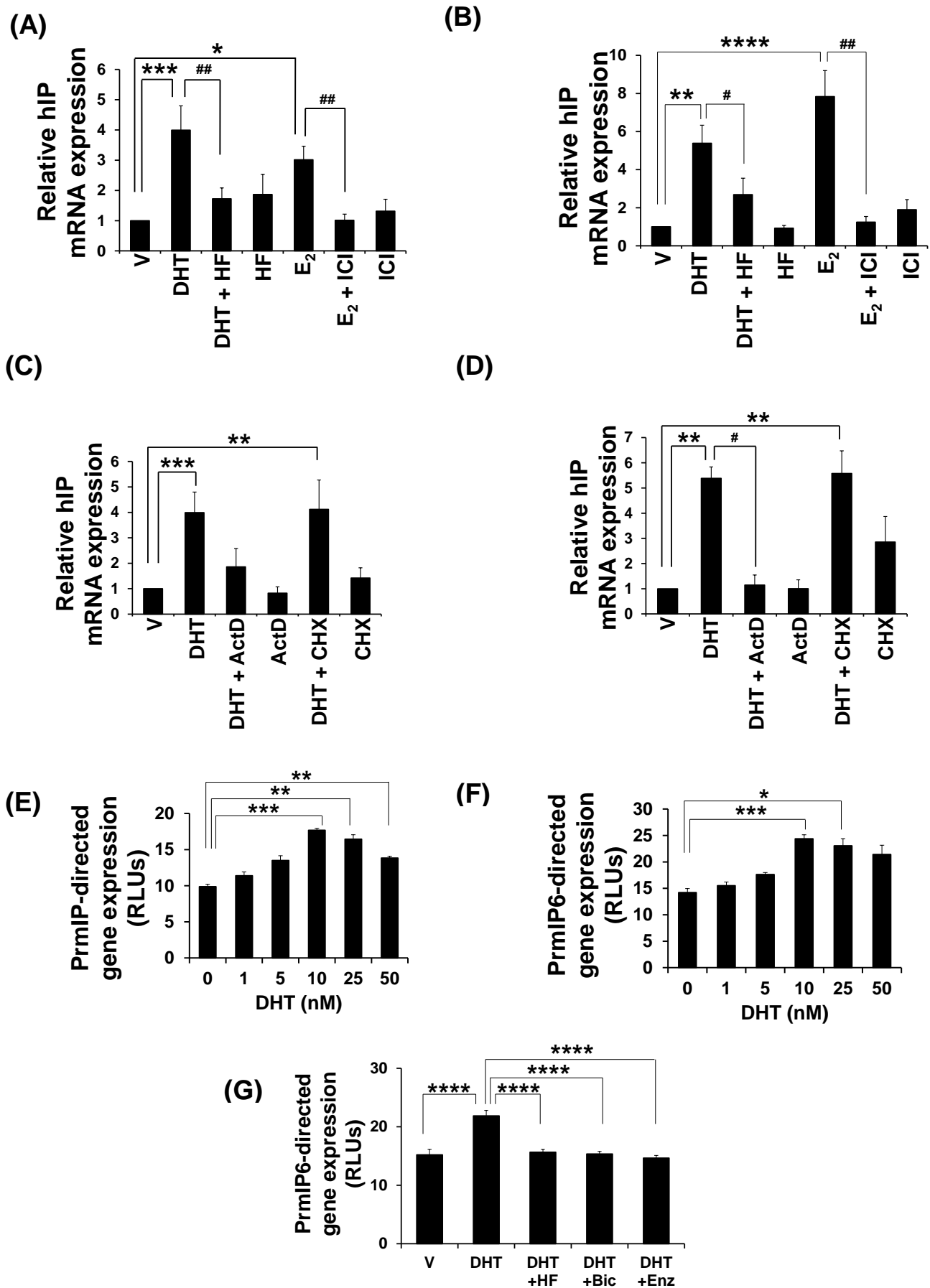
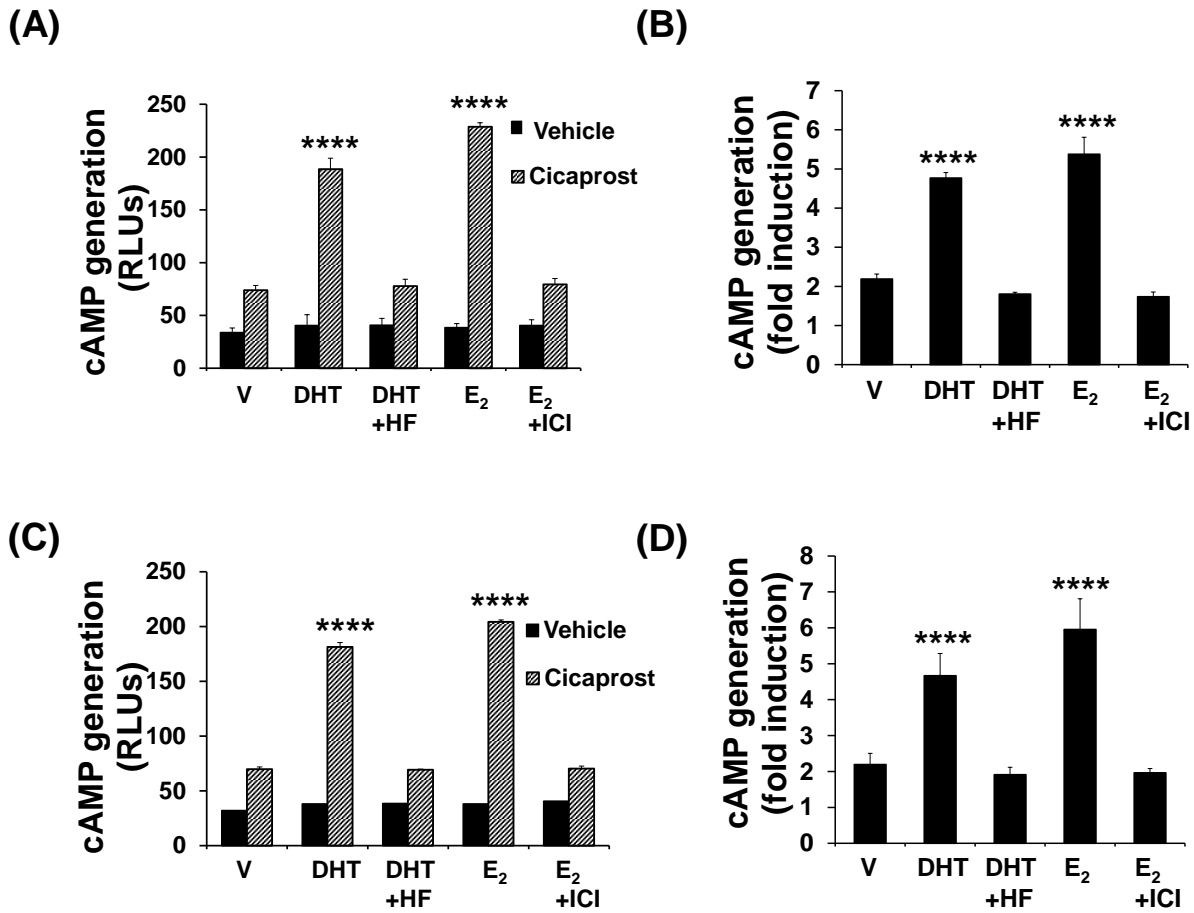
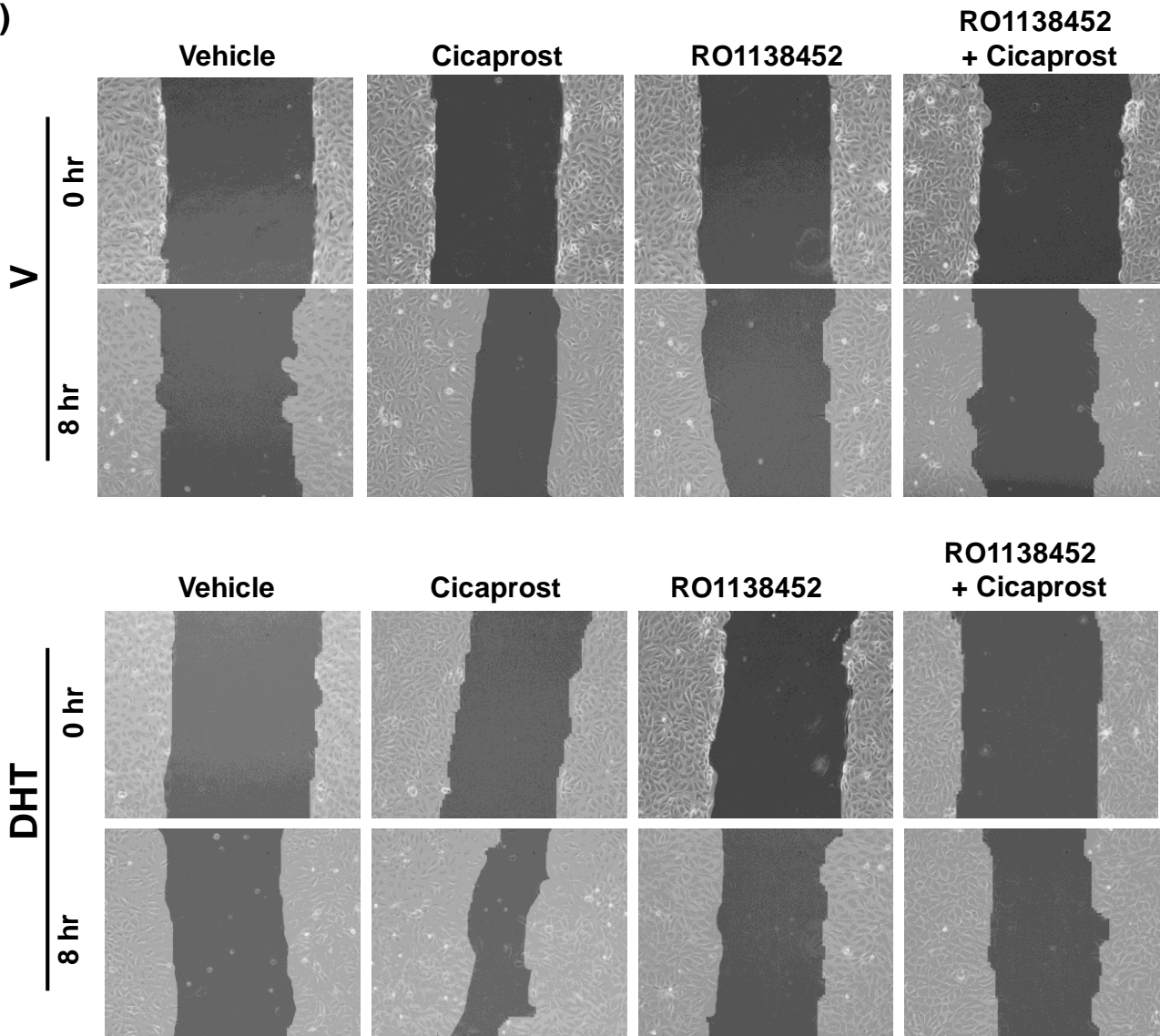


**Figure 2**



(E)



(F)

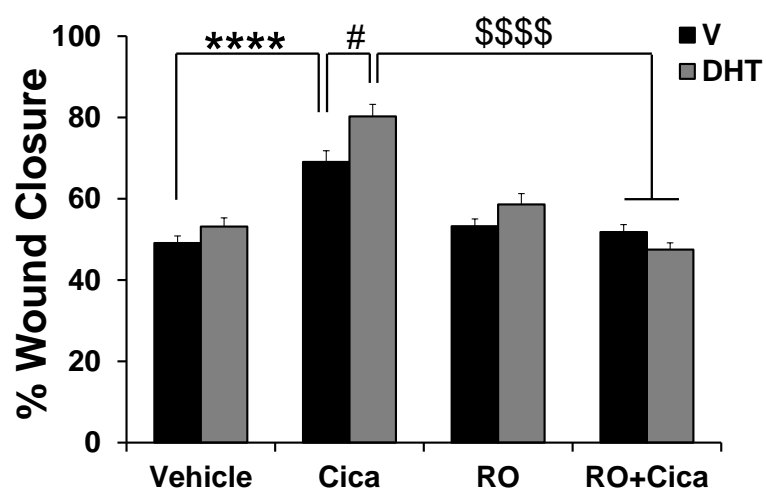
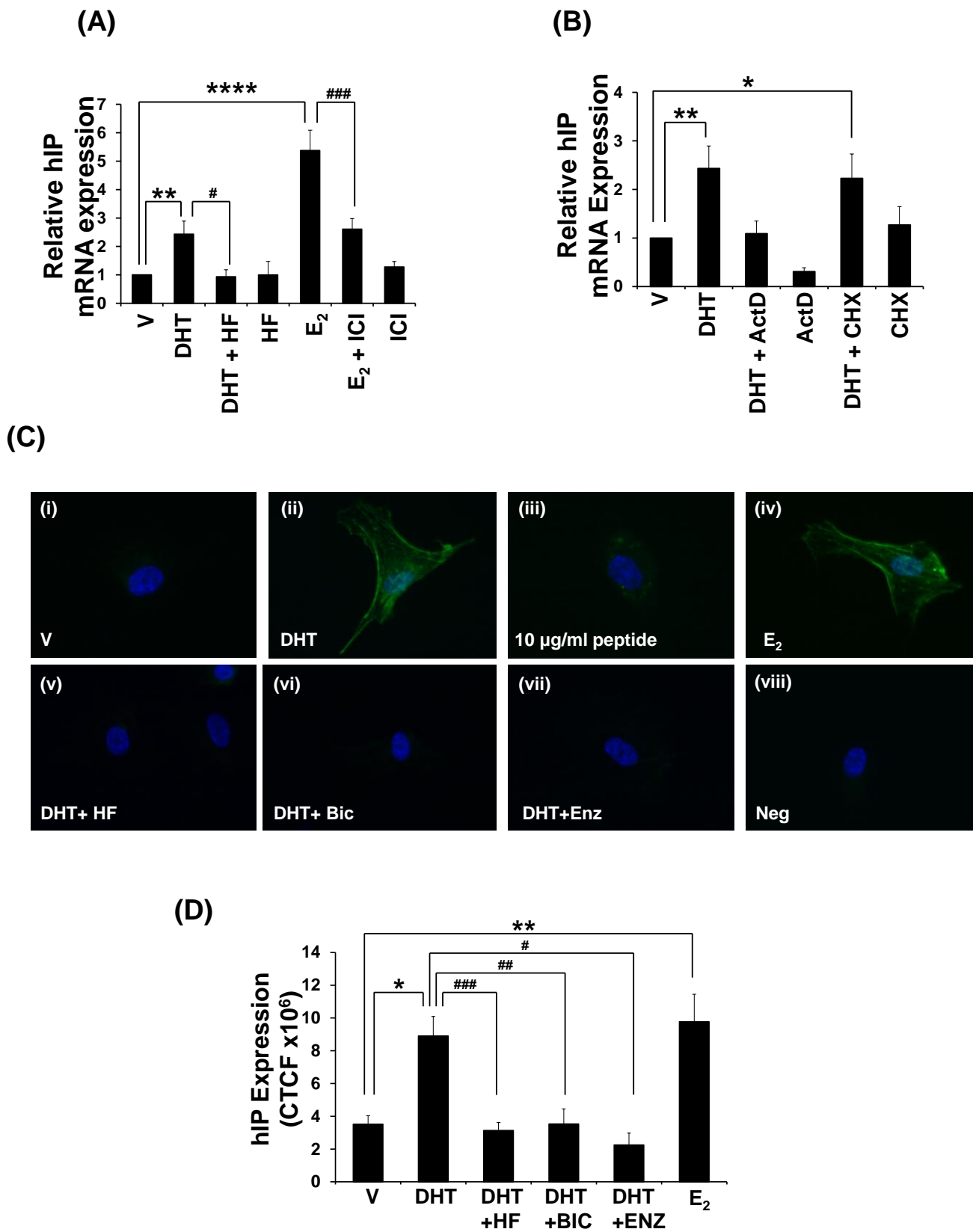


Figure 3



**Figure 4**

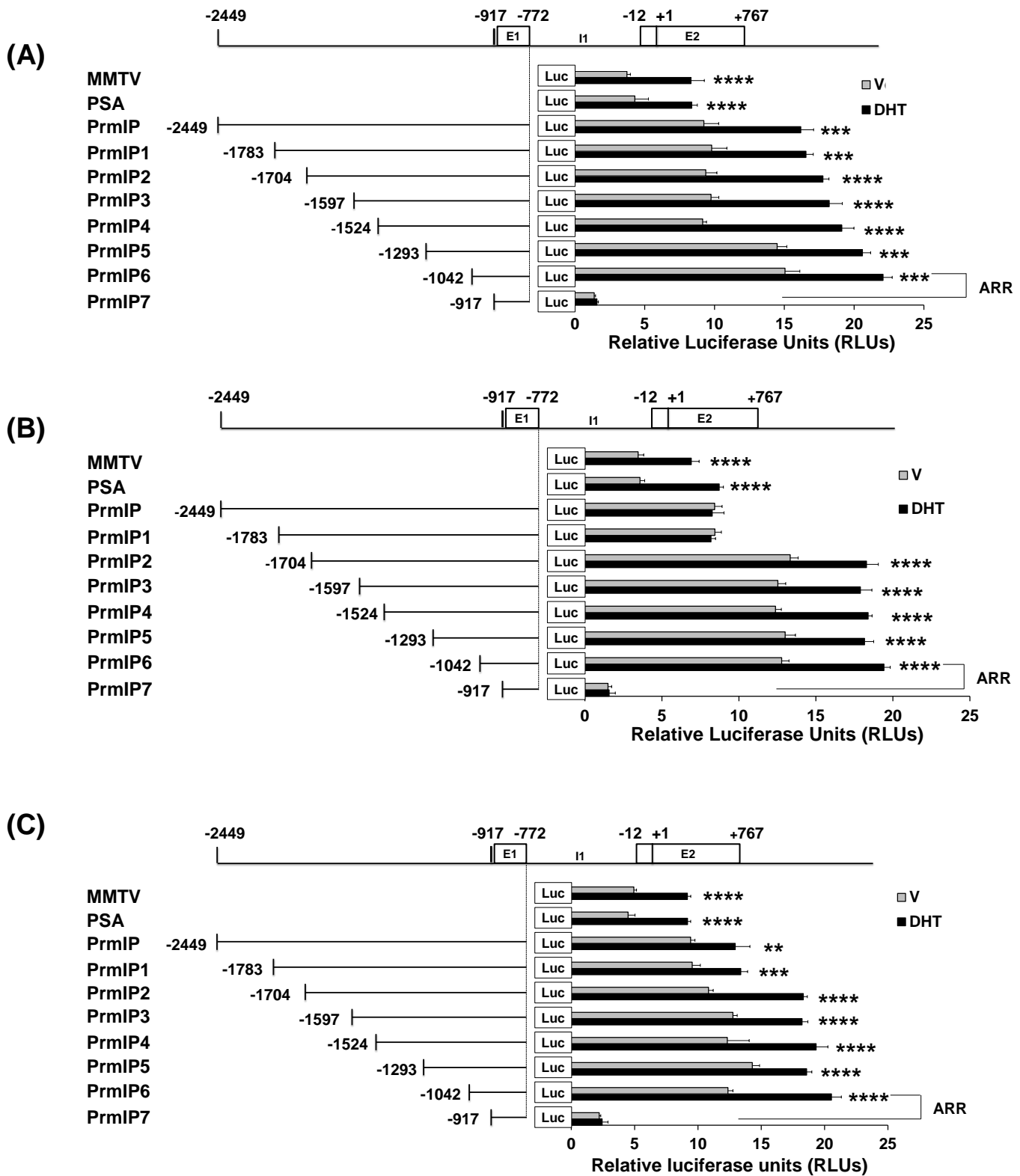
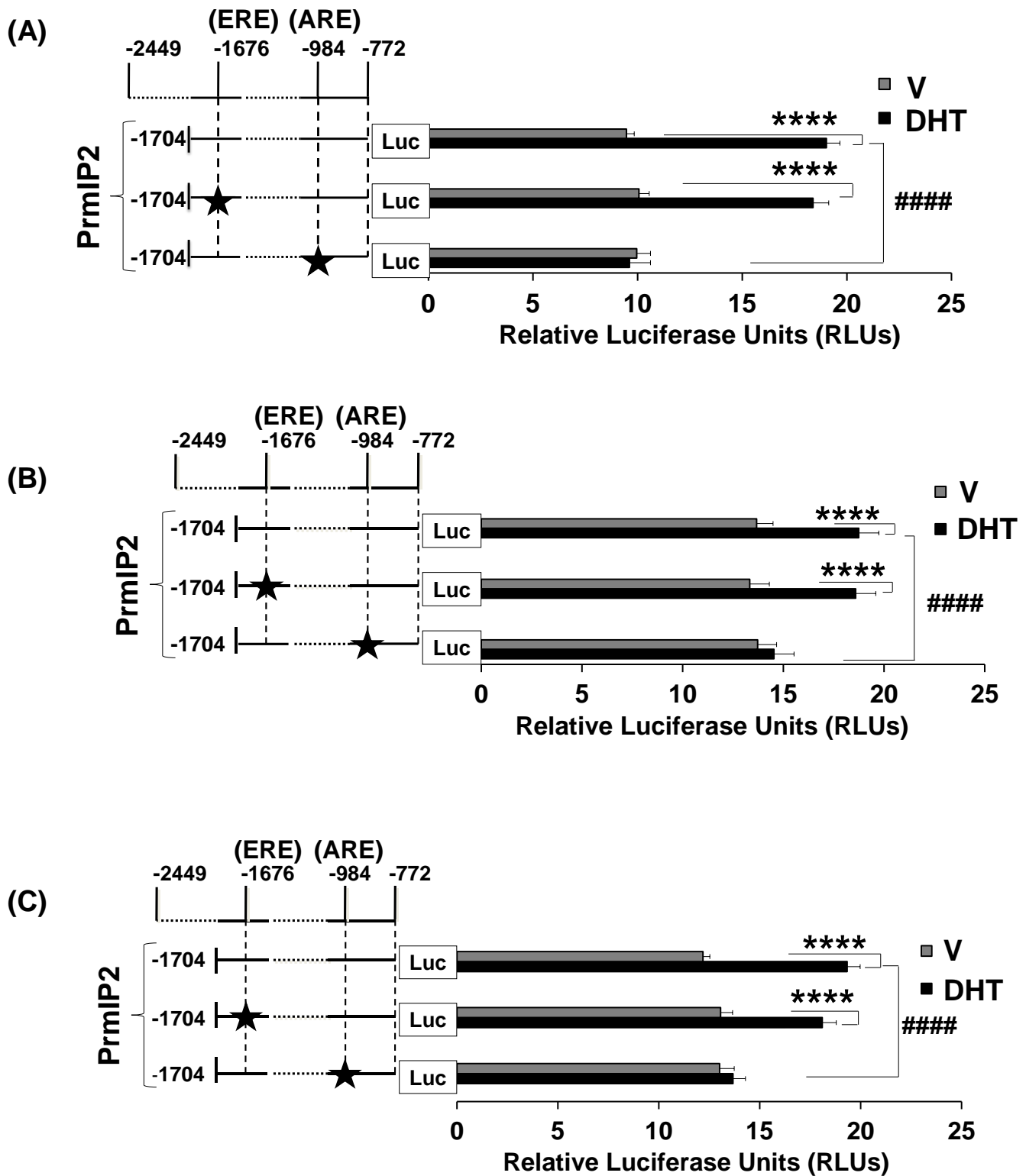
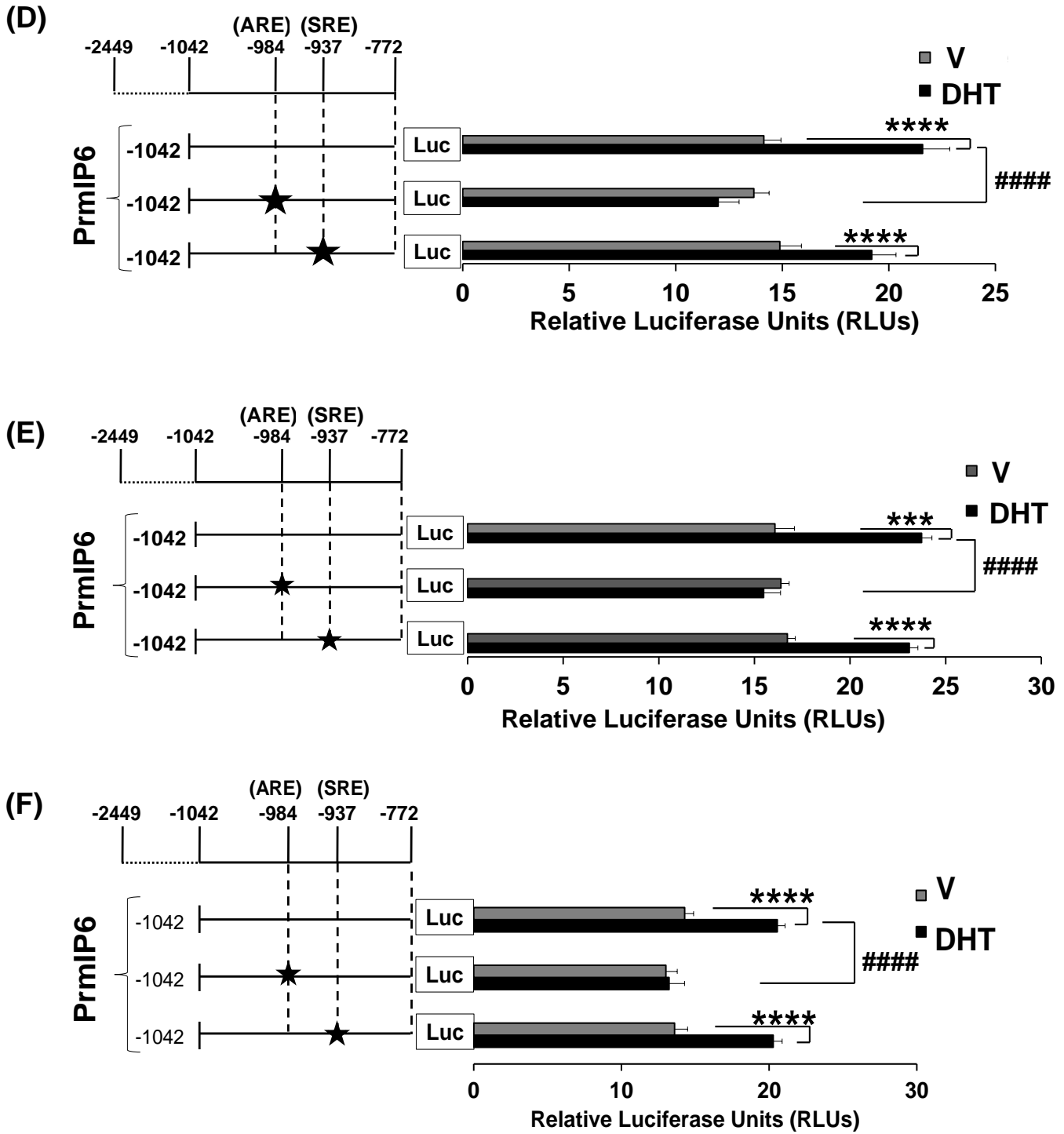
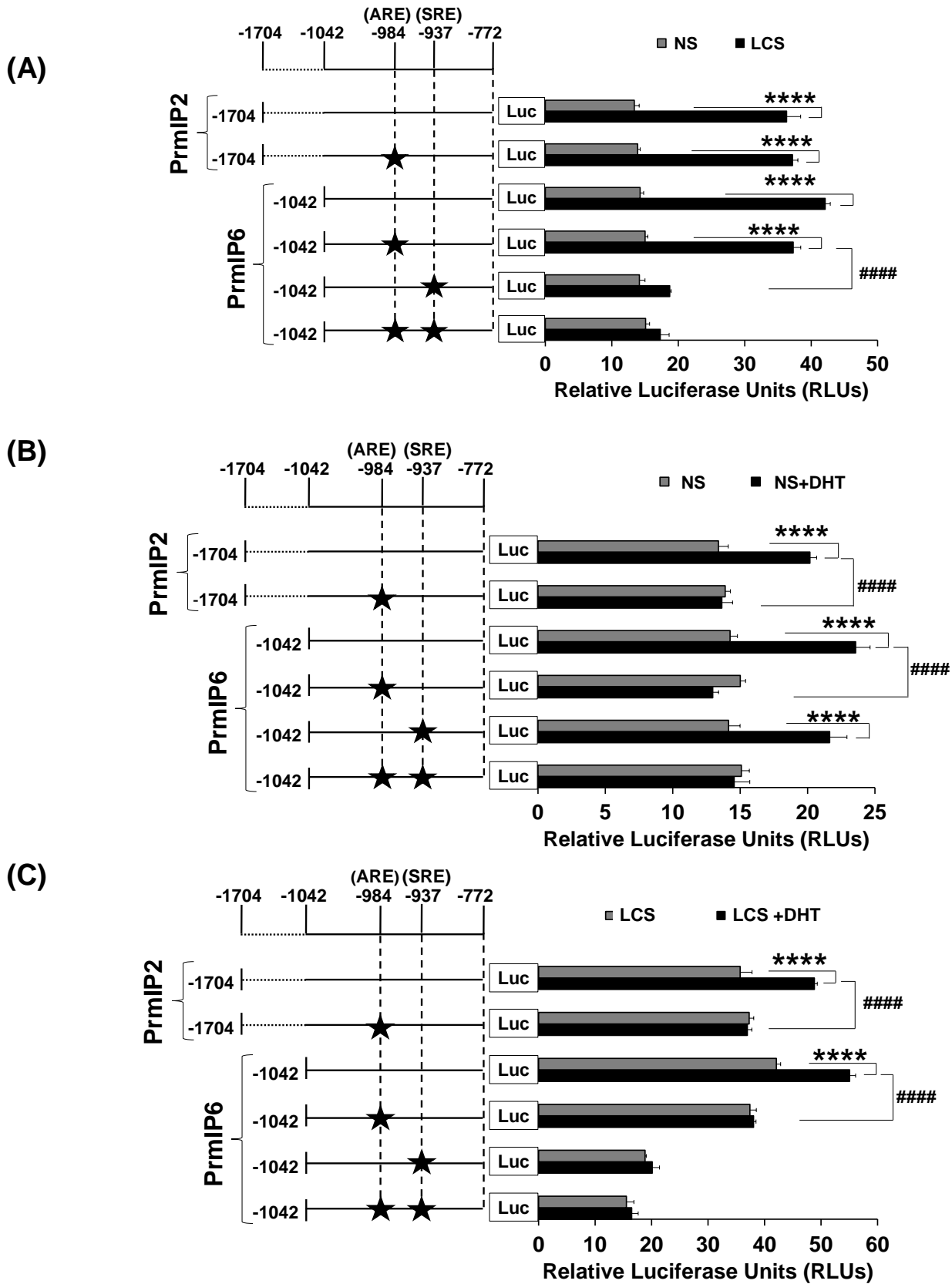


Figure 5





**Figure 6**



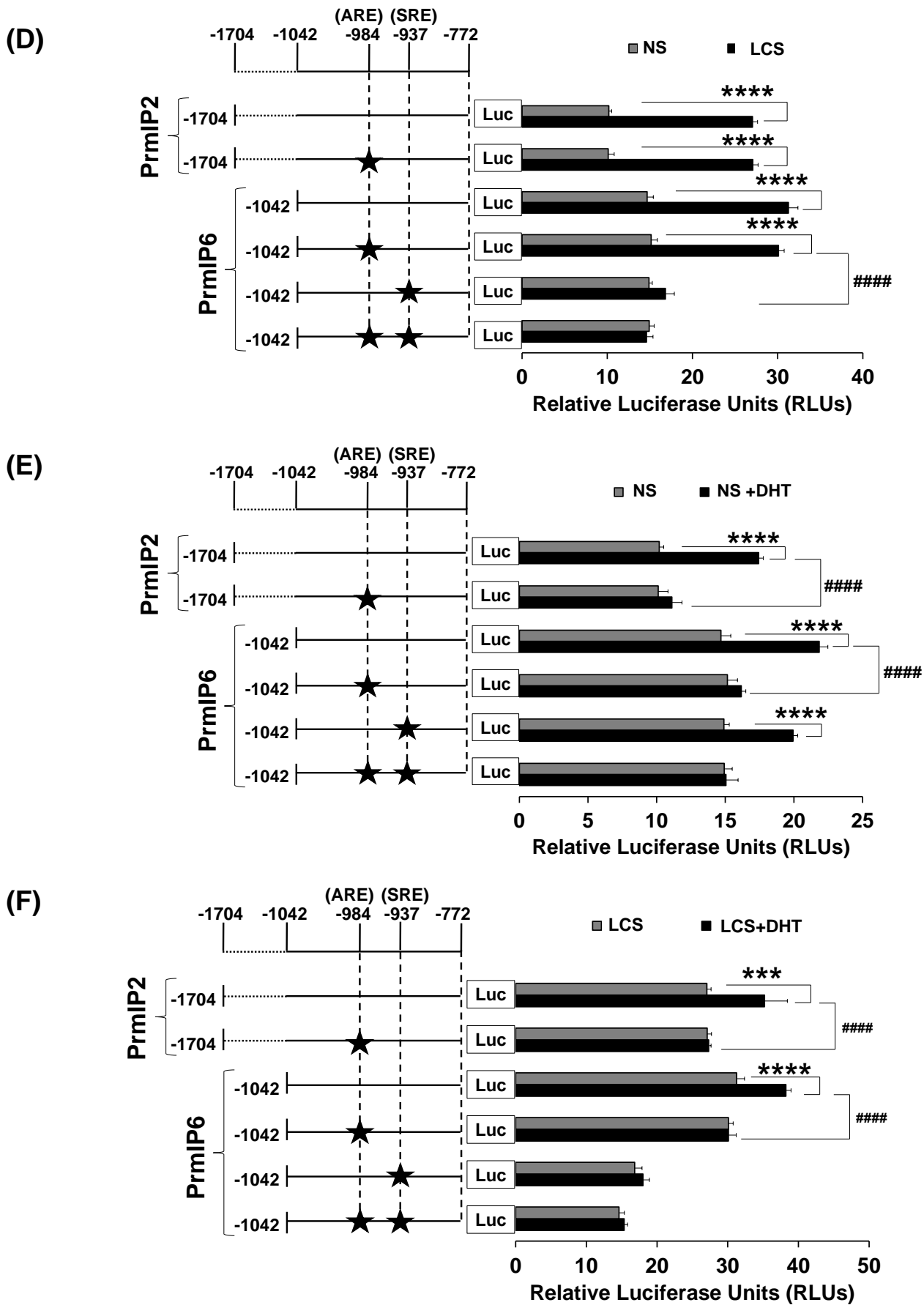
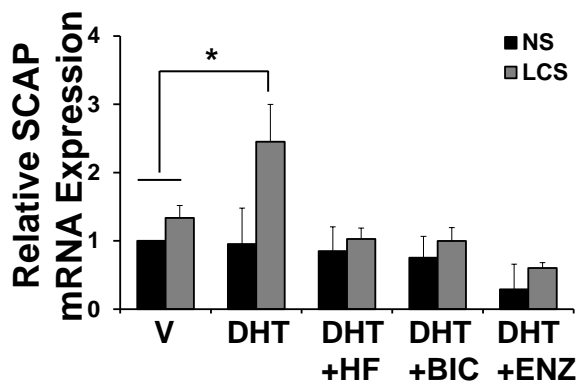


**Figure 7**

**(A)**



**(B)**

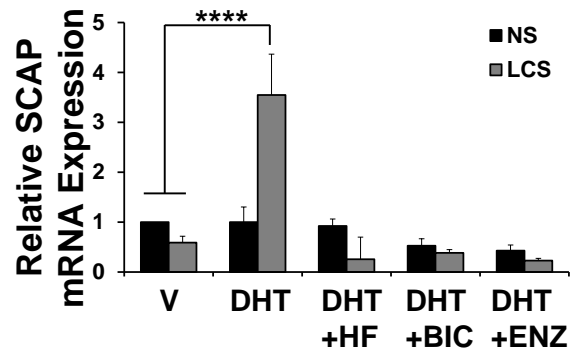
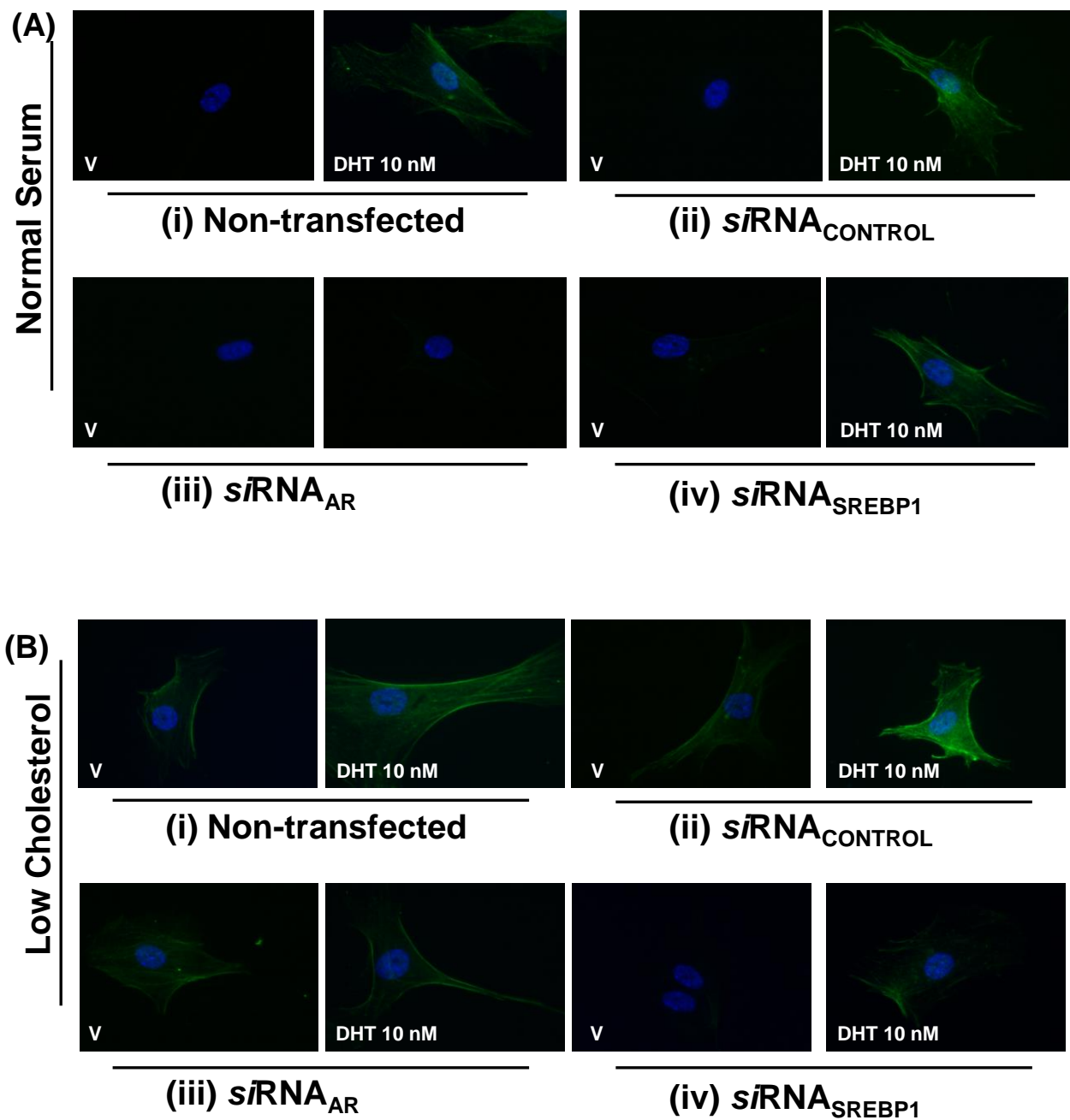
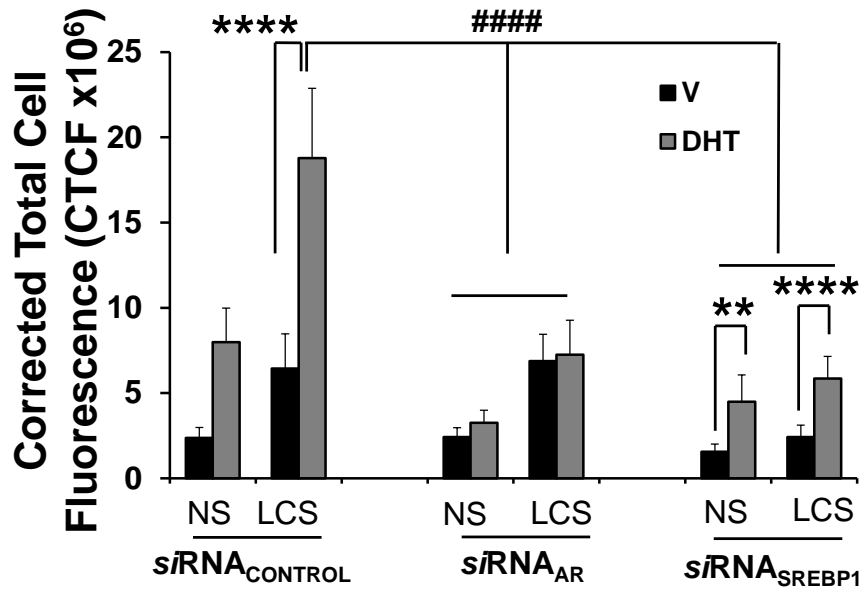


**Figure 8**



(C)



(D)

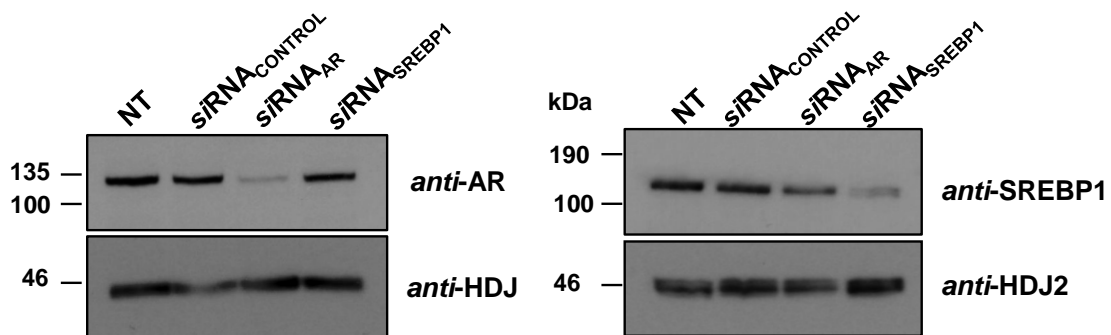


**Figure 9**

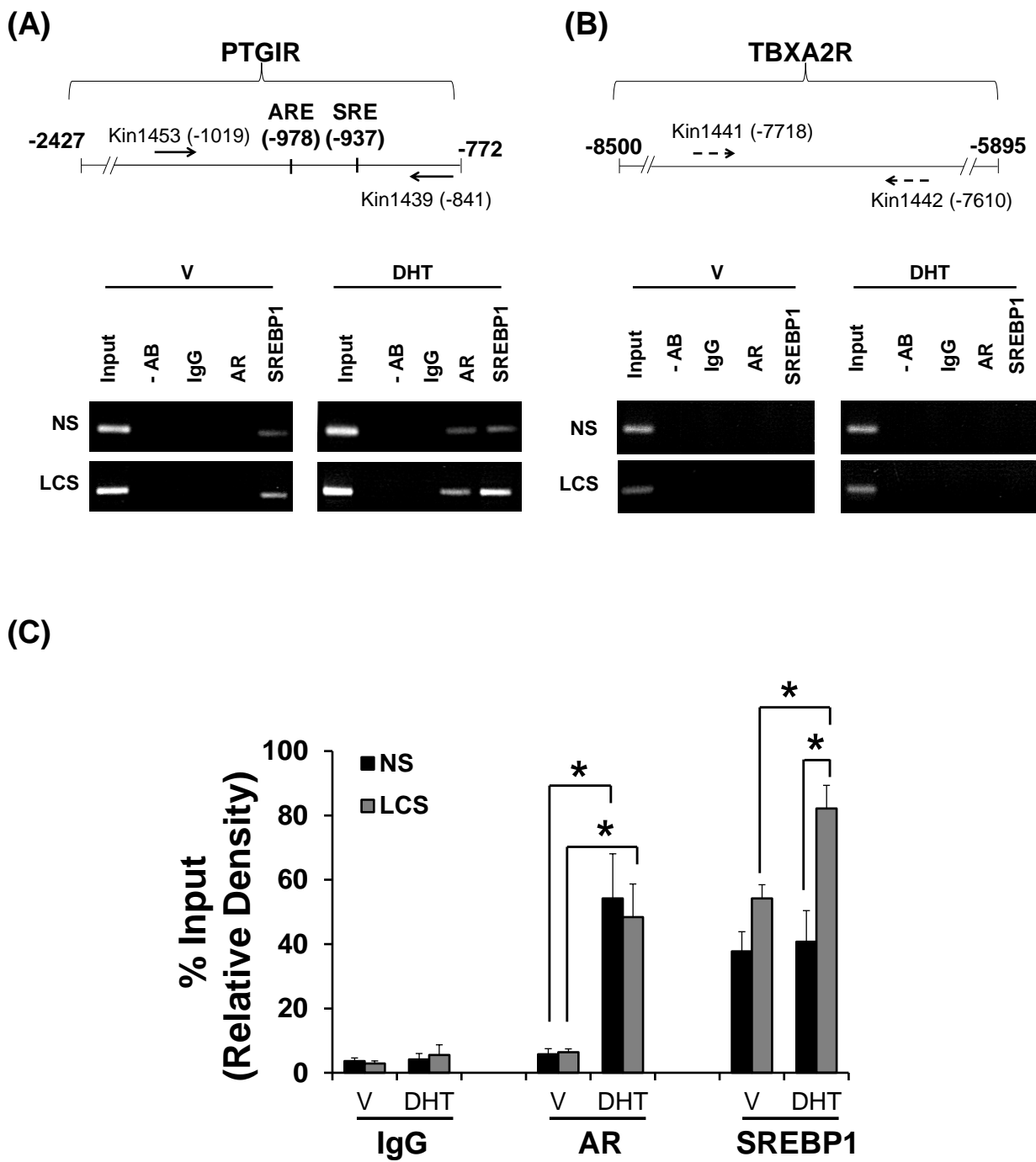
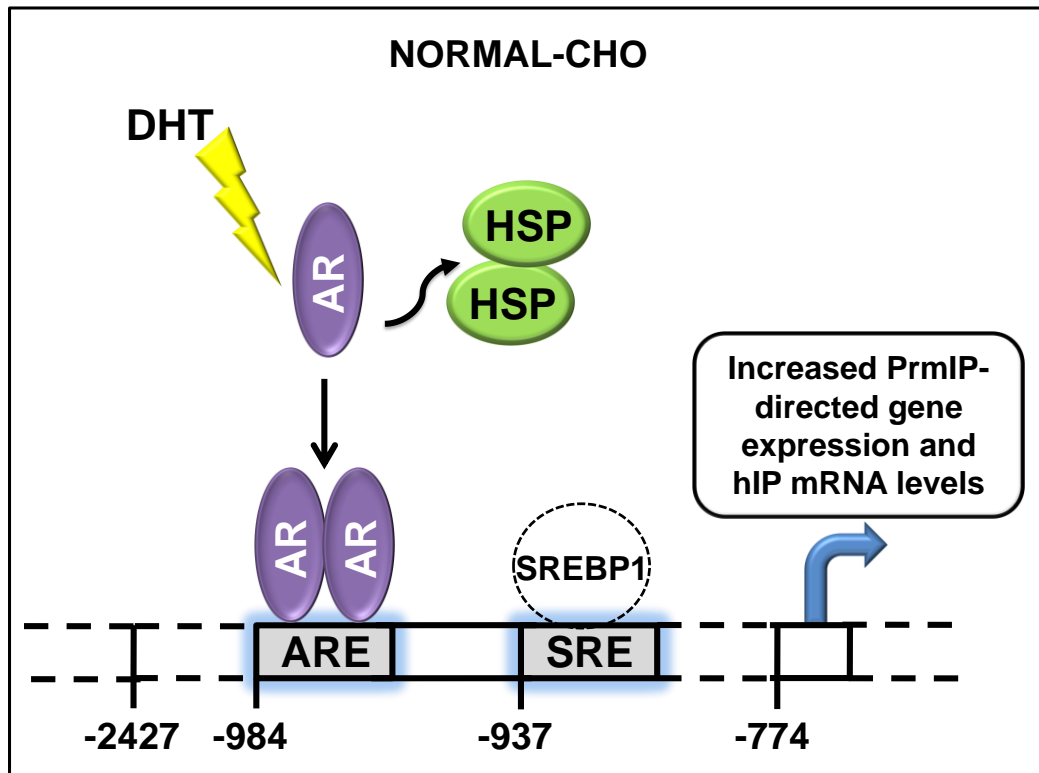
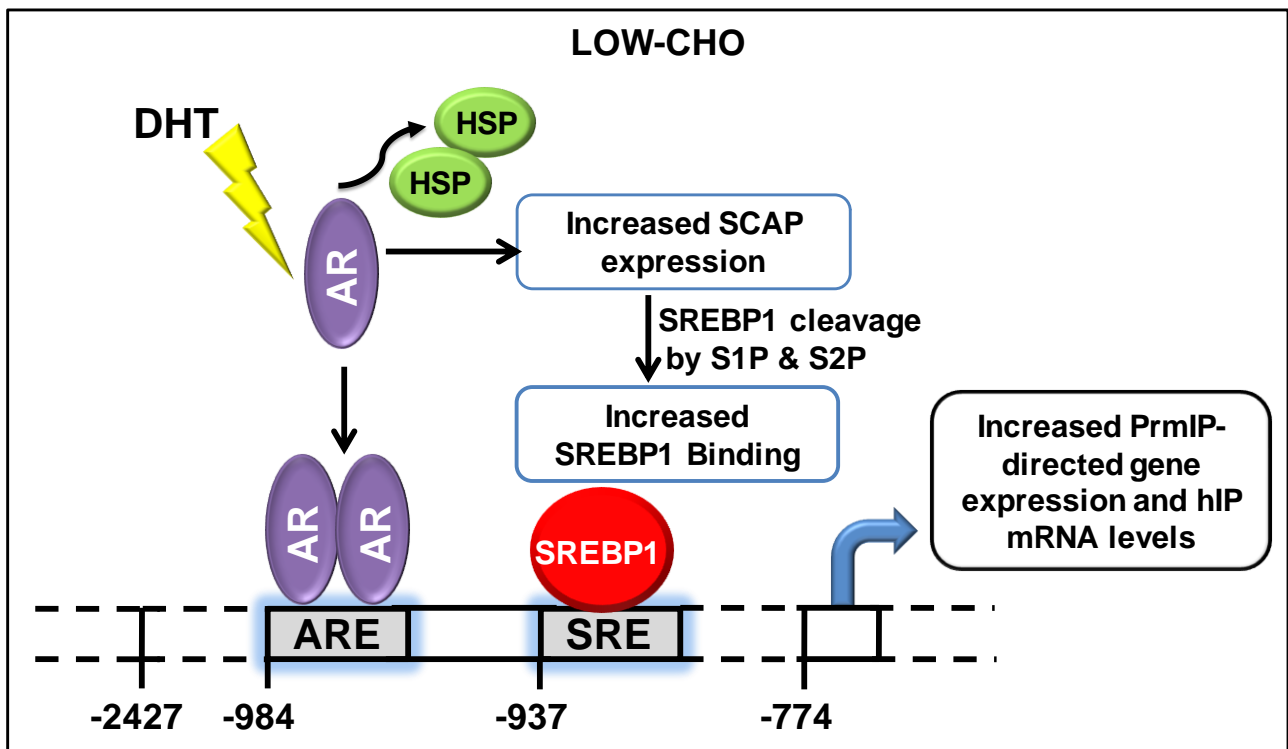


Figure 10

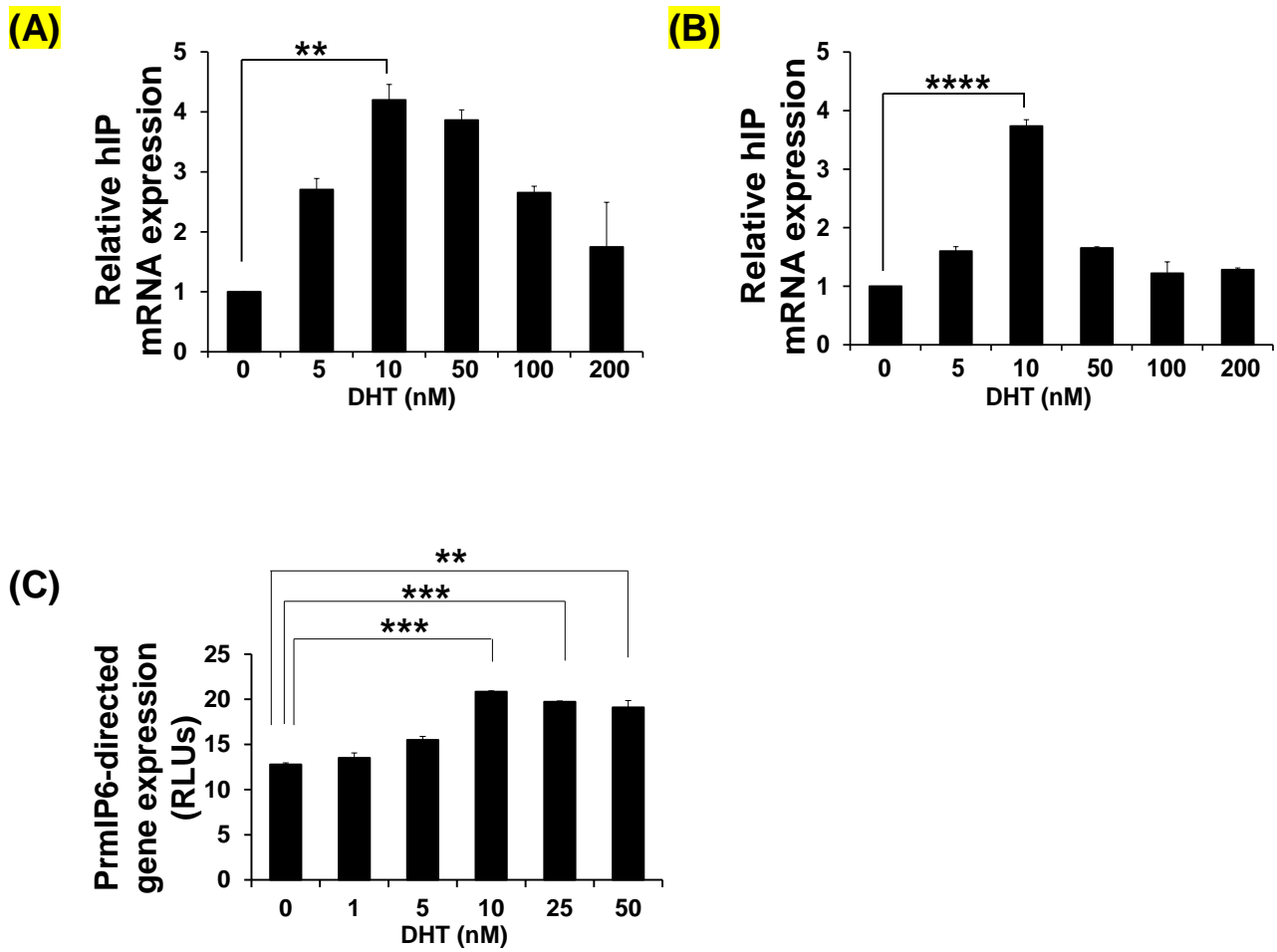
(A)



(B)

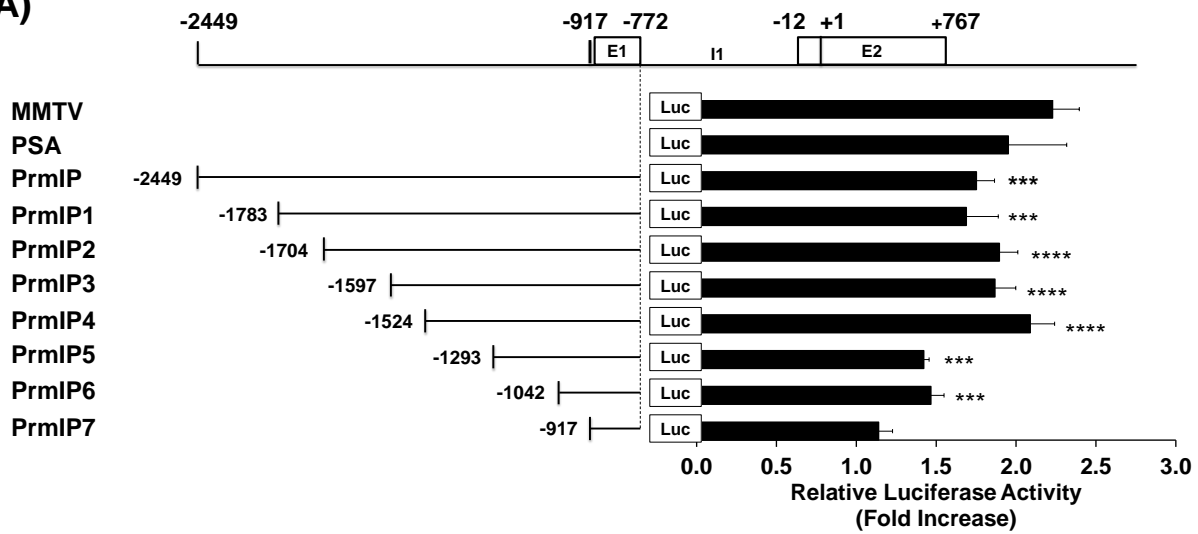


## Supplemental Figure 1

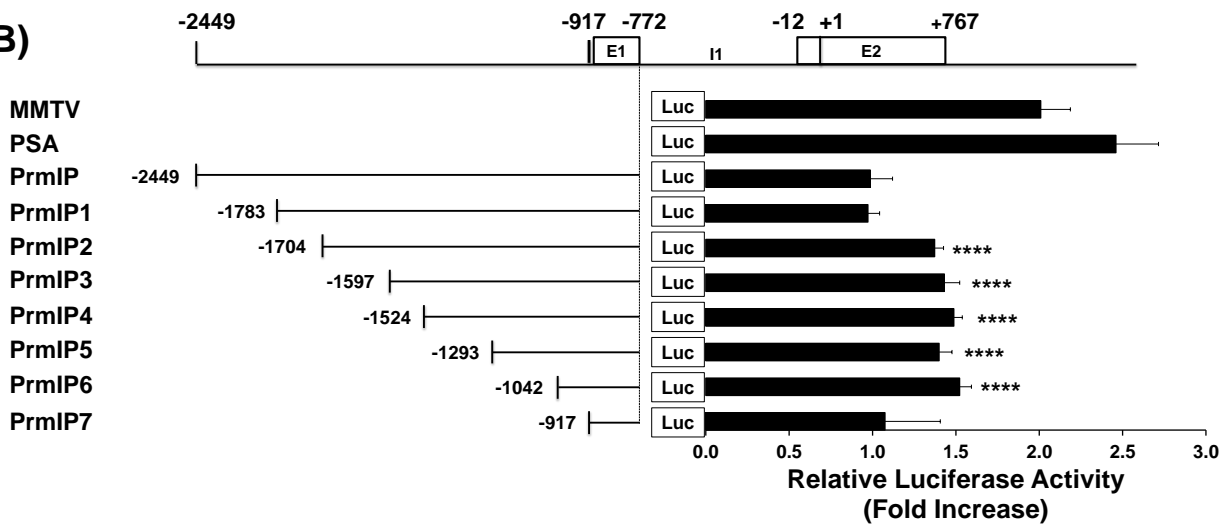


## Supplemental Figure 2

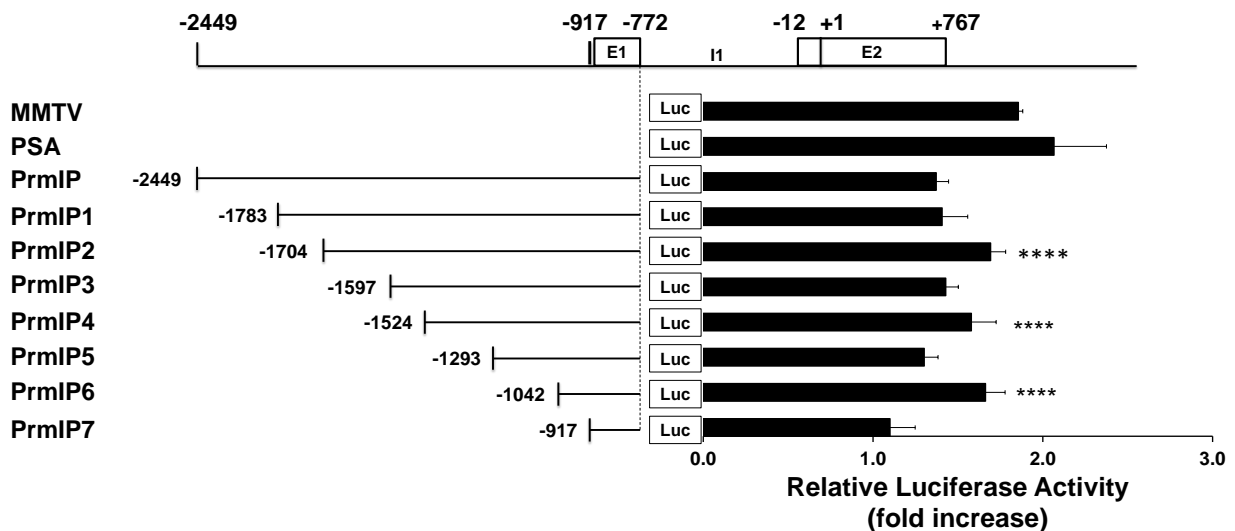
(A)



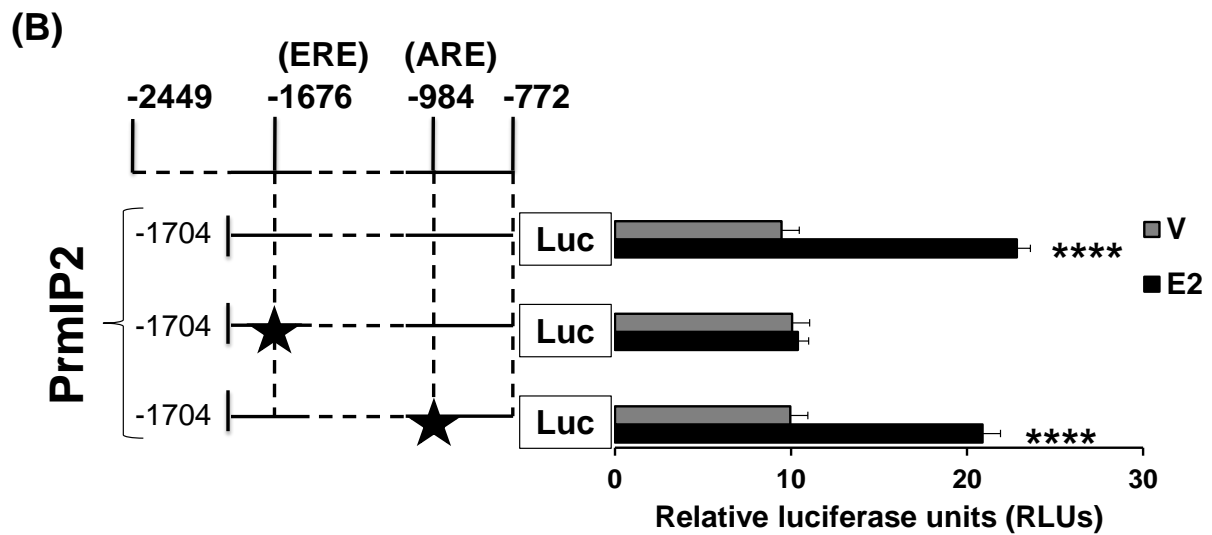
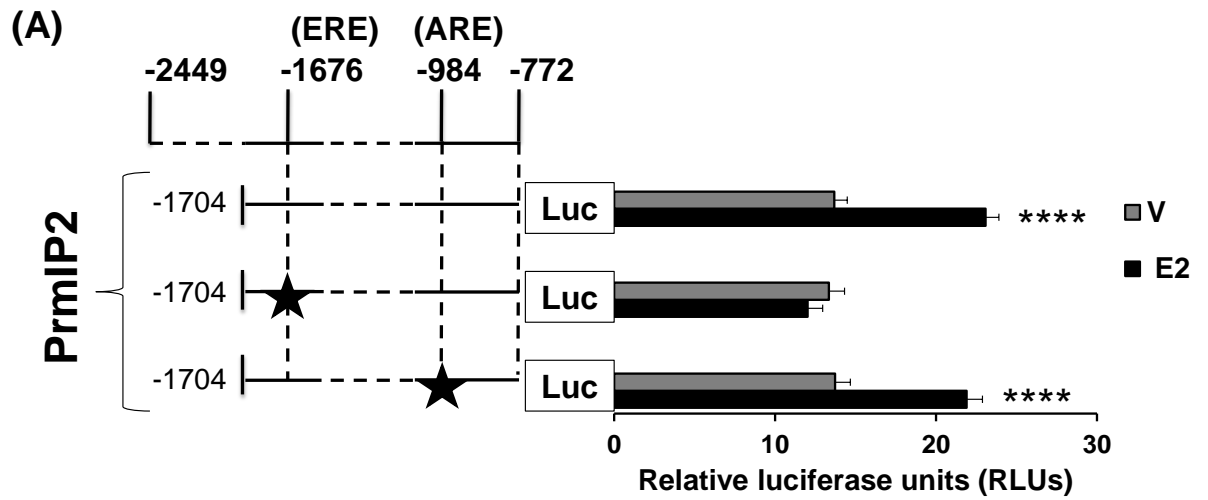
(B)



(C)



### Supplemental Figure 3



### Supplemental Figure 4

